3-11-2011

CubeSat Packaged Electrospray Thruster Evaluation for Enhanced Operationally Responsive Space Capabilities

Scott T. Ober

CUBESAT PACKAGED ELECTROSPRAY THRUSTER EVALUATION FOR ENHANCED OPERATIONALLY RESPONSIVE SPACE CAPABILITIES

THESIS

Scott T. Ober, Captain, USAF

AFIT/GAE/ENY/11-M22

DEPARTMENT OF THE AIR FORCE
AIR UNIVERSITY

AIR FORCE INSTITUTE OF TECHNOLOGY

Wright-Patterson Air Force Base, Ohio

AFIT/GAE/ENY/11-M22

CUBESAT PACKAGED ELECTROSPRAY THRUSTER EVALUATION FOR ENHANCED OPERATIONALLY RESPONSIVE SPACE CAPABILITIES

THESIS

Presented to the Faculty

Department of Aeronautics and Astronautics

Graduate School of Engineering and Management

Air Force Institute of Technology

Air University

Air Education and Training Command

In Partial Fulfillment of the Requirements for the

Degree of Master of Science in Aeronautical Engineering

Scott T. Ober, BS

Captain, USAF

March 2011

AFIT/GAE/ENY/11-M22

CUBESAT PACKAGED ELECTROSPRAY THRUSTER EVALUATION FOR ENHANCED OPERATIONALLY RESPONSIVE SPACE CAPABILITIES

Scott T. Ober, BS
Captain, USAF

Approved:

Lt Col Richard E. Huffman, USAF (Chairman)	10 Mar 11 Date
Lt Col Richard D. Branam, USAF (Member)	3 Mar 2011 Date
Lt Col Carl R. Hartsfield, USAF (Member)	10 Mar 11 Date
Dr. William A. Hargus, III (Member)	3 March 2011 Date

Abstract

This research focuses on the operation of a new specialized electrospray thruster with a potential to be used with a 3-U CubeSat. The key difference in this thruster from traditional colloid thrusters is the porous stainless steel surface used for the emission sites. With this porous surface the actual location and number of the Taylor cones formations vary with changing fuel flow. The understanding of these formations is discussed with low, moderate, and high flow rates. The limitations of the experiment and observed system response are discussed. Due to these limitations, the colloid thruster was only successfully operable in the low mass flow rate regime.

Acknowledgements

Throughout this thesis effort, numerous people have given me overwhelming help and support. My wife, children and extended family: without them, this would not be possible. My faculty advisors, Lt Col Richard Huffman and Lt Col Richard Branam, guided me through each obstacle I encountered. The AFIT laboratory staff always provided me with the tools, experience, and expertise needed. Michael Huggins and Dr William Hargus, my sponsor from the AFRL Propulsion Directorate, supplied the technical materials along with needed advice. I sincerely appreciate everyone's help and appreciate all of the time and effort spent on this project.

Scott T. Ober

Table of Contents

Page

Page

List of Figures

Page

Page

List of Tables

Page

List of Symbols

Symbol	
q	charge of an electron
ε_o	permittivity of free space
R	radius of fuel droplet
m	mass of droplet
ρ	density of the droplet
γ	surface tension
T	thrust
d	distance between charged plates
V	voltage to charged plates
A	Plate Area

List of Abbreviations

Abbreviation	
AFIT	Air Force Institute of Technology
AFRL	Air Force Research Laboratory
CPU	central processing unit
CubeSat	Cube Satellite
DCIU	digital control interface unit
EMI Im	1-ethl-3-methylimidazolium bis(trifluoromethylsulfony)imide ($C_8H_{11}F_6N_3O_4S_2$)
ESA	European Space Agency
GNAT	Geo-orbital Nano-thruster Analysis and Testing
HV	high voltage
LISA	Laser Interferometer Space Antenna
MEMS	microelectromechanical system
NASA	National Aeronautics and Space Administration
PPT	Pulsed Plasma Thruster
PPU	power-processing unit
QRMS-II	Questar Remote Measurement System version two
RF	Radio Frequency

CUBESAT PACKAGED ELECTROSPRAY THRUSTER EVALUATION FOR ENHANCED OPERATIONALLY RESPONSIVE SPACE CAPABILITIES

I. Introduction

The United States Air Force has a great interest in the capabilities of small cube satellites that can perform thruster maneuvers in space. These CubeSats are designed to be small and lightweight: a 1U CubeSat is 10 cm cubed with a mass of up to 1 kg. Air Force Institute of Technology (AFIT) is designing a CubeSat with an integrated propulsion unit. These satellites can perform many missions including: close formation flying with other CubeSats, and possible docking with a large satellite to demonstrate future repair capabilities. These missions are important capabilities that the Air Force desires to develop in the near future.

The electrospray colloid thruster with fuel and an electronics package is contained in a 2U volume, and the thruster requires only 6-8 watts to operate. The promised thrust of up to 1 mN would give this kind of satellite a change in velocity of 200 m/s. This makes the colloid thruster an ideal candidate for the CubeSat.

AFIT and the Busek Company tested a colloid thruster that uses a unique porous emitter to produce thrust by having emissions formed in a range from the droplet regime to the ion cluster regime. This flexibility promises to provide a varying impulse in the range of 200 to 1000 seconds. This research effort attempts to capture the operation of the electrospray thruster through varying mass flow rates of fuel.

This thesis presentation is broken down into five chapters. The first chapter covers the background of colloid thrusters. Chapter two presents a literature review of the colloid technology and principles that allow them to work. The third chapter illustrates the experiments that were performed with the Busek electrospray thruster. Chapter four then expounds on the results of these experiments in showing that this thruster does indeed work. Finally, chapter five presents the conclusions of this thesis.

This chapter will introduce the principles of operation of the colloid thruster. It will give a brief history of the early electrospray experiments and early colloid thruster research. This chapter will also present the recent research in this area and advancements coming about. Finally, it will include the outline of this work, the objectives and contributions to the field.

1.1 What is a Colloid Thruster

A colloid thruster is an electrically powered propulsion system which uses electrical fields to gain mechanical energy in outer space. As with most electric propulsion thrusters, the colloid thruster thrust is attained by electrically accelerating propellant to high speed. Colloid thrusters, as with most electric thrusters, typically offer much higher specific impulse. However, due to practical power source constraints, this thrust is weaker compared to chemical thrusters by several orders of magnitude. Russian satellites have used other types of electric propulsion for decades; even newer Western geo-orbiting spacecraft are using electric propulsion for north-south station keeping. Yet, a colloid thruster has not been utilized in space.

The colloid thruster is an electrostatic accelerator of small charged droplets, clusters of charged molecules or ionic molecules with only a single charge. Figure 1 shows the major components include a power-processing unit (PPU), liquid reservoir, emitter site, extractor electrode, acceleration electrode and a neutralizer. This type of thruster produces thrust in the µN to mN range.

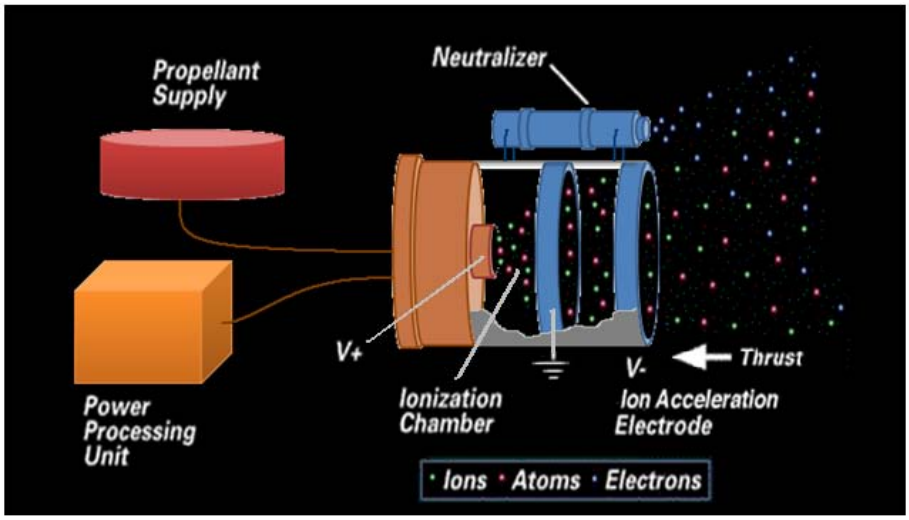

Figure 1. Schematic of an electrostatic thruster

The thrust produced from a single emitter depends on the mass flow rate of the fuel, the velocity of the charged droplet or ion leaving the thruster related to the charge-to-mass ratio and the total acceleration voltage. As with all electrostatic thrusters, the fuel choice is critical for proper performance. New propellants can perform well in the droplet to the ion emission modes, allowing the thruster to have a relatively high thrust or increased ISP depending on the operating conditions.

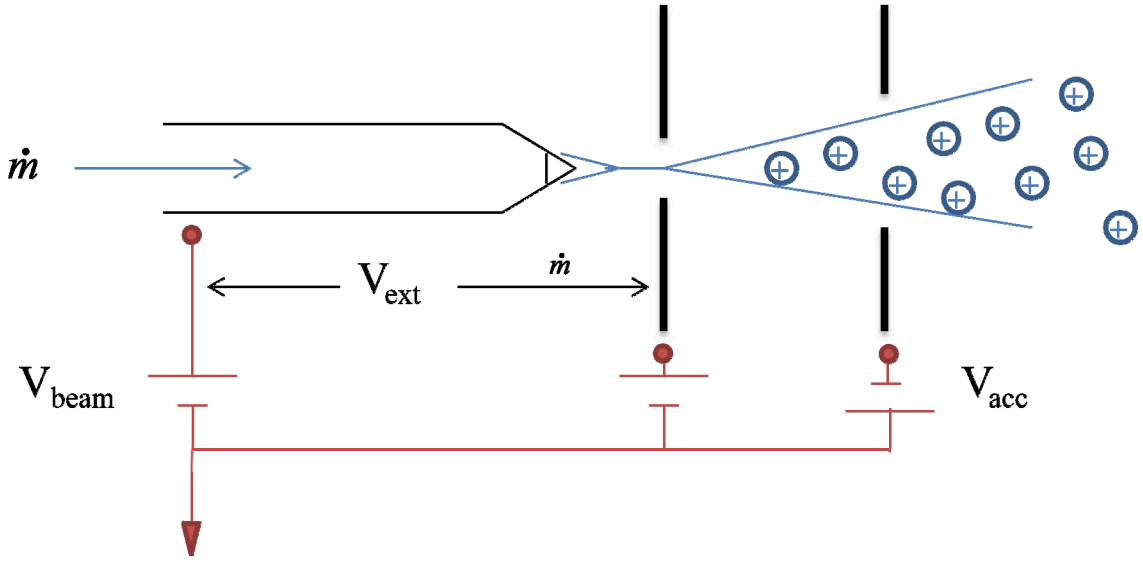

Figure 2. Diagram of a colloid thruster

The major feature distinguishing a colloid thruster from other electrospray thrusters is the need for a neutralizer. The colloid thruster emitting a positively charged plume causes the satellite to build up a net negative charge. This opposite polarity attracts the ions to coat the surface of the satellite.

Without this neutralizer, the satellite body and solar arrays could be coated with the spent propellant, degrading the power system performance due to the covered solar array or outright damage to the satellite itself. The cathode neutralizer emits electrons into the plume, preventing the build-up of any significant electrostatic charge.

The net exchange of momentum occurs with the stream of ionized droplets or ions accelerating out of the thruster by the electric field. With this acceleration of the constituents, an opposite force occurs pushing against this electrical field, creating the thrust in the opposite direction of the droplet stream.

1.2 The First Electrospray Experiments

The first observations of electrosprays were recorded by Zeleny from 1914-1917. His experimental setup consisted of a glass capillary filled with differing liquids (diluted hydrochloric acid, ethanol, glycerin) placed above a grounded plate. The experiment demonstrated that by varying the voltage difference between the liquid and the plate and the pressure of the liquid, a cone formed at the end of the capillary tube [19].

The image on the left of Figure 3 shows the glass capillary 'A' facing a brass disc 'D' serving as the extractor electrode. The liquid pressure was controlled by adjusting the amount of liquid in the glass reservoir 'F'. The wire at 'W' allowed electrical contact to the experimental liquid. The image on the right is the picture taken of the cone with the jet observed on the tip of the capillary by Zeleny. This particular capillary had a diameter of 0.92 mm using liquid ethyl alcohol [19 and 20].

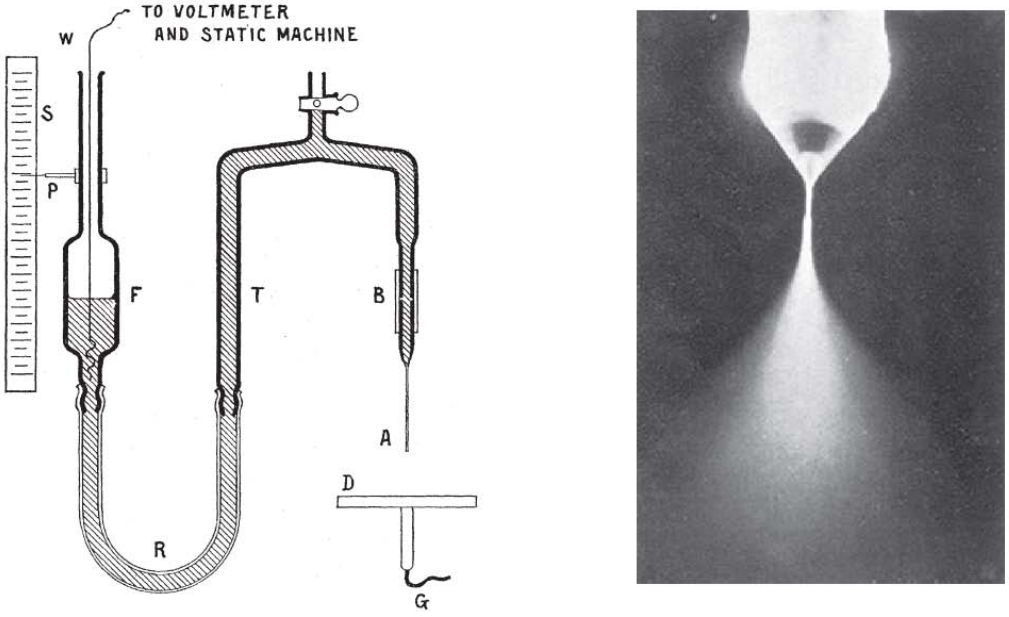

Figure 3. Zeleny's experimental setup and picture of the electrospray [19]

After Zeleny; Macky, English and Drozin continued to study electrosprays with various liquids from the 1930s to 1950s. These experiments helped in understanding that the positive end of the droplet would deform more readily into cone protrusions and that under the right conditions, jet liquid droplets would form.

In 1965 Taylor analytically explained this cone behavior commonly seen in electrospray emitters, called today a Taylor cone. The Taylor cone phenomenon is the surface attraction to the electrical field counteracted by the surface tension in every direction. This balancing between these forces leads to three zones: the cone, the jet stream, and the transition between them.

1.3 Early Colloid Thruster Research

The understanding of the unique Taylor cone formations led to the colloid thruster research in the early 1960s. A great deal of work was devoted to the generation of the charged colloid particle itself. Some particle choices were submicron carbon powder, magnesium oxide, or even capturing condensation from an homogeneous vapor. All these efforts fell short in performance compared to the electrospray emitter.

During this same decade, the United States Air Force began a systematic effort to identify a propellant that would work when the jet is negatively charged. This work identified what an electrochemical criterion of the metallic electrode must have in relation to the ions in the propellant. TRW Inc., also working with a negative charged jet, performed a parametric study using a single needle emitter. In a joint venture, the Air Force and TRW Inc. built a bipolar thruster prototype having both positive and negative

emitters working simultaneously. Concerns resulting from the experiment were hydrogen bubble formations and arching.

As the years of research went by the requirements of the fuel choice, shape of needles used to create Taylor cones and material choice for the cathode were refined. The United States Air Force even launched a flight qualification program for a complete colloid thruster system. In 1974, this program tested a 432-needle prototype with the key performance as shown in Table 1 [18].

Table 1. Performance of 432 needle colloid thruster prototype, taken from Urdiales [18]

Performance Area	Value
Thrust	4.4 mN
Specific Impulse	1365 s
Power	70 W
Efficiency	58%
Needle Voltage	12.2 kV
Extractor Voltage	-2.3
Specific Charge	12500 C/kg
Extractor Current	25μA

One major issue with the early thrusters was the degradation of performance by the 1000 hours of operation. Erosion and deposition problems were observed, modeled and with future designs were overcome. The greatest hindrance to the colloid research came at the end of the 1970s with the budgetary cutbacks caused by the new space shuttle program. The United States government abandoned the colloid thruster research and development.

1.4 Recent Research & State of the Art

Since that time, a need has developed for finely controlled maneuvering in space experiments in mapping the earth's gravitational fields. NASA Jet Propulsion Laboratory has developed a space qualified colloid thruster in a short time, starting with a first breadboard in 2001 to a qualified flight model delivered to the European Space Agency (ESA) in 2008 to fly on the NASA LISA mission. LISA, the Laser Interferometer Space Antenna, is a joint NASA–ESA mission to observe astrophysical and cosmological sources of gravitational waves of low frequencies in space. The use of the colloid thruster is ideal in the required fine thrust corrections needed to maintain the perfect distances between the three satellites as they orbit around the earth [15].

The newly gained interest in this technology is also linked to the effort to miniaturize satellite systems. Electrospray propulsion systems are easier to miniaturize, have high efficiencies and specific impulse. Although research on electrospray thrusters had disappeared in the west for almost thirty years, the use of electrosprays for mass spectrometry of large organic molecules popularized the technology and made components such as needles or other components readily available [5].

Investigating novel fuels has expanded the list of liquids with the ability to be purely ionic spray. Other advantages of ionic liquids are good electrical conductivity, no measurable vapor pressure, and a spray capability at either positive or negative voltages. The newest on the list is the EMI Im, an ionic liquid having high efficiency in the ionic and droplet emission modes [1].

The research into creating the Taylor cones for the colloid operation is breaking down into three broad areas. The first is the use of needles in creating the Taylor cone at

the tip of the needle. This was the original method in early experiments, as was described in sections 1.2 and 1.3. In preparation for the NASA DRS-ST7 mission, a colloid thruster is now space certified. The use of needles in forming the Taylor cones is the most used in current research projects on colloid thrusters.

The next area of technology in colloid thruster research is the use of micro-needles within a microelectromechanical system (MEMS) to produce the Taylor cones. The basic premise is to shrink the thruster down to the point of operation on a small chip. It uses the same principles as the needle colloid thruster but miniaturizes the thruster in order to place many of them on the same chip. This technology could greatly improve the overall performance from the same volume as compared to the traditional-sized needles. One major hurdle with this technology is the tendency of the thruster to short out and destroy itself in a relatively short time. The system short out is due to the close proximity of the high voltage differences required in the operation of the colloid thruster [9].

The last method of creating the Taylor cones is the use of a rough surface or a porous emitter instead of traditional needles. The research to improve the capillary feeding of the fuel by utilizing a rough surface was pioneered in the early 1960s. This research developed the use of a porous emitter allowing the thruster to run at a greater thrust range by varying mass flow rates of the ionic fuel. This variable flow rate creates a change in the number of Taylor cones formed from the porous emitter surface. With the other two methods in the colloid thruster, the mass flow rate of the fuel and the chosen extraction voltage controlled the charge-to-mass ratio by adjusting the size and shape of the Taylor cone jet. With a fixed extraction voltage, increasing the flow rate of the fuel

leads to an increase in thrust. This lowers the charge-to-mass ratio of the emitted droplet. Thus with less interaction with the electric field, the specific impulse decreases as well [4].

Only the Busek Company and AFIT have completed any work with this technology and their results are within this thesis. With the use of the porous surface, each multiplex emitter can create thousands of Taylor cones emission sites. With this method of creating the electrospray, the thruster is throttled by varying the voltage and/or the mass flow rate of the fuel. This variance changes the colloid thruster operation from an ionic emission to a droplet mode, in turn changing the ISP from 1000-4000s down to 300-2000s using the same ionic fluid and emitter surface and producing up to 1mN of thrust.

1.5 Thesis Objective

The objective for this thesis is broken down into four parts. The first part is to operate a colloid thruster in the AFIT vacuum chamber labs. This entails integrating the Busek Electrospray thruster and electronics into the lab, creating the mounting structures, and installing instrumentation so that research is performed and recorded. It also includes refining the user manuals so follow-on research students can run the equipment. Second, ensure that the colloid thruster is operating properly by comparing operation at the Busek facility and at AFIT. Third, capture the flow patterns of this thruster, from the droplet domain to ion domain. Fourth, explore the operating envelope of this specific thruster and measure its performance. By accomplishing these goals the thruster operation will

have occurred outside of the manufacturer's facilities, a big accomplishment with cutting edge technology.

The testing from this thesis resulted in a enhanced understanding of this unique colloid thruster. From this colloid, the Pulsed Plasma Thruster (PPT) and micro-Hall thrusters research can provide a more informed decision of which propulsion unit should best be integrated into the school's 3U cube for future missions. These missions include maintained orbit in space for longer durations, close formation flying with other cube satellites and possible docking with a large satellite to demonstrate future repair capabilities. These are all important mission capabilities the Air Force desires to develop in the near future. Each of these missions requires a propulsion system to be part of the cube satellite. This colloid thruster and an electronics package could be contained in a 1U volume, and low power requirements would be ideal. The promised thrust of up to 1 mN would give this kind of satellite a change in velocity of 200 m/s.

II. Literary Review

The purpose of this chapter is to describe the understanding of colloid thrusters today. First, the chapter will present the mission and the performance requirements of this thruster. Next, it will present some major elements that affect the performance of the colloid thruster and some of the formulas that describe their performance. Then, it will present the performance of the colloid thruster with thrust, specific impulse, and efficiency.

2.1 Colloid Thruster Operation

The colloid thruster is an electrostatic accelerator of small charged droplets, clusters of charged molecules or ionic molecules with only a single charge. Major components include liquid reservoir, emitter, and an extractor electrode.

The thrust produced from a single emitter depends on the mass flow rate of the fuel, the velocity of the charged droplet or ion leaving the thruster, the charge-to-mass ratio and the total acceleration voltage. The fuel choice is critical for proper performance. New propellants now can perform well in the droplet to the ion emission modes allowing the thruster to have a relatively high thrust or increased Isp depending on the operating conditions.

The emitter for the colloid thruster supplies the conductive fluid to the strong electric field, in orders of 10^5 to 10^6 V/m. A balance between the surface tension and the supplied electronic field results in the formation of Taylor cones. At the tip of the Taylor cone is a stable stream of charged droplets continuing to accelerate by the same electronic field.

Current state of the art electrospray thrusters are capable of producing μN up to mN of thrust. These thrusters can operate in the 200s - 1000s specific impulse. It is estimated that newer ones could reach up to 4000s. The choice of emitters has been limited to wet capillary needles with new research into nano-sized emitters. A new emitter design by the Busek Company uses a porous substrate for the emitter allowing the formation of thousands of Taylor cones from a 7.2mm^2 area.

2.2 Droplet vs. Ionic Emission

Colloid thrusters use Taylor cone emission sites to produce a combination of singularly charged ions and charged droplets. The fractional amount of one versus the other is dependent upon the following factors: the emitter surface characteristics, the propellant physical properties, mass flow rate, and the extraction electrical field strength.

The colloid operating in the charged droplet mode is well understood whereas the ion emission mode has only been demonstrated in the laboratory under controlled conditions. To have a thruster operating in both regimes is a major technical challenge. One of the limiting factors is the capillary needle commonly used to create the Taylor cone spray condition. The needle works well with forming liquid droplets but does not function well in forming the singularly charged ions or clusters.

With the emitter aligned with the extraction and acceleration grids, the stainless steel porous substrate, a very small surface area can create thousands of Taylor cones due to the surface characteristics by adjusting the applied voltages and fuel flow rates. This capability allows the colloid thruster system to operate in both ionic and droplet regimes with the same thruster head, electronics, and feed system.

2.3 Droplet Size and Charge

From the physical nature of the Taylor cone, the fuel, as it progresses to the tip of the jet, maintains equilibrium of forces on the surface between electrostatic attraction to the field and surface tension. The balance is disrupted at the tip of the jet formation but the energy potential is maintained. The energy captured is related to its radius found in the following equation.

$$q = 8\pi(\varepsilon_o\gamma)^{1/2}R^{3/2} \qquad \text{Eq. 1}$$

Where q is the fundamental electon charge, ε_o is the permittivity of free space, γ is the liquids surface tension and R is the average radius of the droplet. The droplet mass is

$$m = \frac{4}{3}\pi R^3\rho \qquad \text{Eq. 2}$$

The ρ is the density of the liquid. The charge rate to mass is then the following equation.

$$\frac{q}{m} = \frac{6(\varepsilon_o\gamma)^{1/2}}{\rho R^{3/2}} \qquad \text{Eq. 3}$$

The above equations represent the Rayleigh limit, the largest charge per unit mass supported by a droplet of a defined radius. The minimum energy in the formation of the droplet in the Taylor cone is exactly half of the maximum value. In the real world, the charge per unit mass is closer to the lower limit. This makes the more accurate equation of charge per unit mass to be:

$$\frac{q}{m} = \frac{3(\varepsilon_o\gamma)^{1/2}}{\rho R^{3/2}} \qquad \text{Eq. 4}$$

2.4 The Fuel

The choice of fuel in this colloid thruster thesis is 1-ethl-3-methylimidazolium bis(trifluoromethylsulfony)imide ($C_8H_{11}F_6N_3O_4S_2$) called EMI Im. The room temperature ionic liquid propellant is being flight tested for the NASA DRS-ST7 mission. This propellant, which has passed all space environmental exposure tests, has excellent properties in both droplet and ionic thruster operation [15].

The fuel mass flow controls the charge-to-mass ratio by adjusting the size and shape of the Taylor cone jet. With a low mass flow rate, the fuel forms the Taylor cones on the sharp feature of the porous emitter. This regime forms the ion clusters allowing the thruster to operate at higher Isp. At higher mass flow rates, the fuel Taylor cones form through the interaction of the surface tension of the fuel and the electrical field. At this state, the fuel emits from the surface as droplets. The greater mass of the droplet leads to increased thrust from the thruster.

2.5 Mass Flow Rate

The mass flow rate of the fuel controls the charge-to-mass ratio by adjusting the size and shape of the Taylor cone jet. With a low mass flow rate, the fuel forms the Taylor cones on the sharp feature of the porous emitter. This regime forms the ion clusters. This allows the thruster to operate at higher Isp.

At higher mass flow rates, the Taylor cones form by the interaction of the surface tension of the fuel and the electrical field. At this state, the fuel comes out as droplets. These heavy droplets compared to the ions allow the thruster to produce more thrust.

The mass flow rate determines the charge. With a large percentage of formations, being charged droplets, the flow rate decreases and the cone jet becomes smaller, allowing the charge-to-mass ratio to increase while the current from the emission site decreases. With the power of the emitter held constant, the number of Taylor cone sites must increase to compensate for the decrease in mass flow and current being carried by each individual site.

If the mass flow decreases further, the power of the electric field increases, leading to the emission sites attaching directly to the solid porous surface. Consequently, the surface size and shape play an important role in determining the type and amount of emissions. With the surface designed to have sharp surface features, adjusting the electric field with a steep gradient and having low flow rates produces purely ionic emissions. These transitions are possible by controlling the flow rate of the fuel.

2.6 Mass Flow Rate Interaction with Taylor Cone Formations

What makes this transition possible is the porous emitter. The porous stainless steel surface used to create the electrospray thrust is different from traditional needle electrospray thrusters. The use of the porous emitter allows the thruster to run at a greater range of varying mass flow rates of fuel. This variable flow rate creates a change in the number of Taylor cones and is believed to be formed at different locations on the surface of the thruster. The theory of a porous surface thruster in operation is broken down to three different phases: low, moderate and high flow operations.

For traditional colloid thrusters, the mass flow rate of the fuel and the chosen extraction voltage control the charge-to-mass ratio by adjusting the size and shape of the

Taylor cone jet. With a fixed extraction voltage, increasing the flow rate of the fuel leads to an increase in thrust. This lowers the charge-to-mass ratio of the emitted droplet, thus with less interaction with the electric field the specific impulse decreases as well.

With a porous surface there is an added level of complexity, the ability to form additional Taylor cones with the varying mass flow rate. These cones can form at many different locations on the surface compared to the traditional emission site that is formed at the end of a needle. The following figure and paragraphs explain further the difference in a porous surface electrospray thruster.

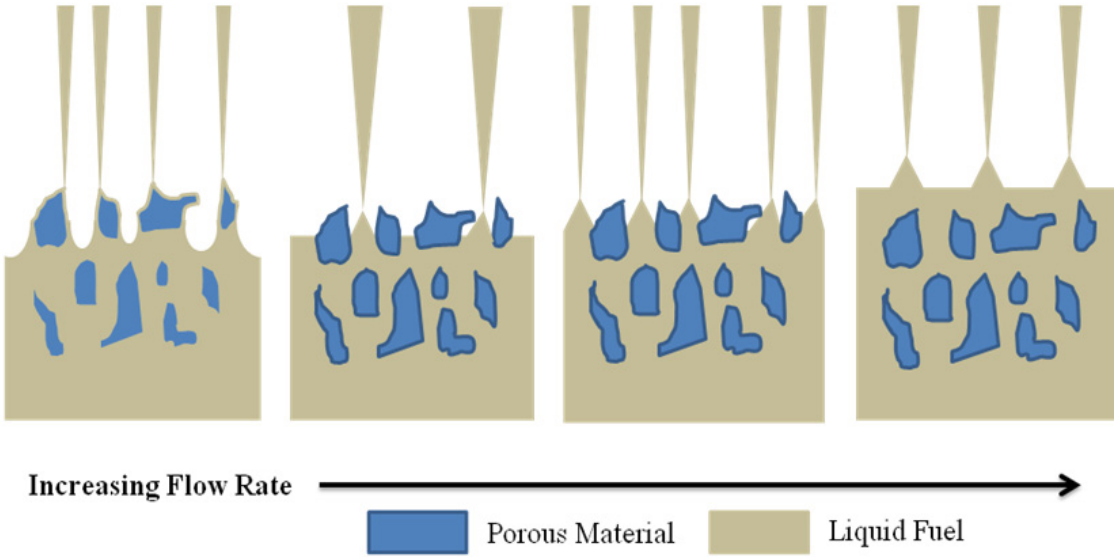

Figure 4. The change in the emitter sites as liquid fuel flow increases.

Figure 4 illustrates the effect of the electric fields on the ionic fuel as the rate of this fuel increases from left to right. As this fuel rate increases the number of Taylor cone formations and there location changes. The porous emitter surface represents the blue and the gray represents the liquid ionic fluid.

As seen in Figure 4 first tile, the low mass flow rate of the fuel, the force of the electrostatic field pulls the ionic fluid to the closest points of the surface. The Taylor cones form on the sharp feature of the porous emitter. In this regime, the propellant is extracted as ion clusters instead of droplets. These ion clusters allow the thruster to operate at a higher Isp than traditional colloid thrusters, but at a lower thrust.

At moderate fuel flow rate represented in Figure 4 second and third tiles, the electric field overcomes the surface tension, allowing the Taylor cones to anchor to the porous voids in the surface. As the fuel rate increases, additional Taylor cones form in the smaller voids of the surface. At this state the fuel comes out more as droplets than ions. The greater mass of these droplets leads to increased thrust from the thruster. In this region of operation, the thrust output relation to the flow rate corresponds with that of a traditional colloid thruster.

At high flow operation shown in Figure 4 the last tile, the total porous surface is flooded and the surface features no longer anchor the Taylor cones. It is theorized the emission sites become so dense that each site starts to electrostatically shield neighboring sites. This leads to a maximum number of Taylor cones which can be formed on the surface of the fuel. With the maximum number of emitter sites formed, any further increase in flow rate leads to larger mass flow per emission site, thus increasing the thrust while reducing the specific impulse of each site. At this state, the fuel comes out as droplets. The greater mass of these droplets leads to increased thrust from the thruster.

2.7 Electrospray Thruster Performance

The colloid thruster falls under the principles of electrostatic acceleration. The interrelations of the electrical and dynamic forces are calculated by limiting these forces to one-dimension. With a porous substrate used to create the emitter site, some of the calculations are then adjusted due to the possible droplet to ionic operating regimes.

In this characterization of a thruster, three fundamental items are important to know. First, the specific impulse of a thruster is equivalent to the miles per gallon for an engine. From the specific impulse value, the average exit velocity of the ionic substance out of the thruster is calculated. The second characteristic is the acceleration force (thrust) which a thruster can produce. The last characteristic is the efficiency of the thruster to produce the kinetic thrust energy.

The first fundamental idea, the specific impulse is the measure of energy content in the fuel and its conversion efficiency into thrust. The specific impulse is defined by

$$I_{sp} \equiv \frac{T}{\dot{m} g_o} = \frac{v_e}{g_o} \qquad \text{Eq. 5}$$

Where T is the thrust, $\dot{m}$ mass flow rate, g_o is gravitational acceleration of the earth, and v_e is the exit velocity of the ion. For electrostatic propulsion systems, the exit velocity is a function of the kinetic energy of the ion to the potential voltage, V_a, of the electric field that accelerates the ion.

$$v_e = \sqrt{\frac{2V_a q}{m}} \qquad \text{Eq. 6}$$

The above equation is for the ideal liquid. A different equation is used when working with actual fuels. With fuel properties taken into effect, the exit velocity becomes the following equation.

$$v_e = \left(\frac{2V_a f(\varepsilon)}{\rho}\right)^{1/2} \left(\frac{K\gamma}{Q\varepsilon}\right)^{1/4} \quad \text{Eq. 7}$$

Where ε is the dielectric constant, K is conductivity, and Q is the volumetric flow rate of the liquid fuel. The function $f(\varepsilon)$ is dimensionless and found by experimental data for the specific fuel case.

Propellants with high values of conductivity correlate to high specific impulse values. The limit to the specific impulse maximum is the molecular weight of a single propellant molecule or the weight of a charged cluster. Ionic liquids which form small clusters or have a lower molecular weight also lead to higher specific impulse values.

The second fundamental idea for thruster performance is thrust. The thrust of any thruster is defined by the following relationship.

$$T = \dot{m}v_e = \sum n\sqrt{2V_a mq} \quad \text{Eq. 8}$$

The n represents the number of ionized constituents. For a thruster to achieve higher values of thrust, an increase of mass flow rate, or increase of the exit velocity is needed. Increasing the thrust decreases the thruster's specific impulse value.

When calculating the thrust for the colloid thruster with a varying number of emitter sites use the following equation.

$$T = C_n I_B^{3/2} V_a^{1/2} \quad \text{Eq. 9}$$

Where I_B is the beam current and C_n is a constant based on the propellant properties. With the variable number of emitting sites, C_n is found by the following equation.

$$\dot{m} = \frac{C_n^2}{2} I_B^2 \quad \text{Eq. 10}$$

$$C_n = C_1 \sqrt{\frac{n_1}{n_n}} \quad \text{Eq. 11}$$

Here C_1 is the thruster constant and n_1 is the number of emission sites which correlate to this constant. With the number of emission sites on the surface of the emitter varying with respect to the flow rate, leads to range of values for C_n.

The last fundamental of thruster performance is the thruster efficiency. The propulsive efficiency (η_{th}) of an electrospray thruster is the propulsive power divided by the input power.

$$\eta_{th} = \frac{T^2}{2\dot{m} I V_a} \quad \text{Eq. 12}$$

ṁ is the mass flow rate of the liquid and I is the current being used by the thruster. The current is related to the mass flow rate times the charge per unit mass. This gives the equation

$$I = \frac{\dot{m} q}{m} = \sum nq \quad \text{Eq. 13}$$

With the above relation equation 11 is written as

$$\eta_{th} = \frac{T^2}{2\dot{m} I V_a} = \frac{\left(\sum n \sqrt{2 V_a m q}\right)^2}{(2 V_a \sum nm)(\sum nq)} \quad \text{Eq. 14}$$

The above equation assumes all ions will be the same mass. In reality with the emitter creating varying sizes, the ions accelerate to different speeds. An exhaust stream containing more than a single speed is a less optimal arrangement compared to all particles going the same speed. The increased energy required to accelerate the faster particles or droplets is larger than the extra thrust derived from these faster constituents.

The method to find the actual efficiency of a built electrospray thruster is to measure the thrust force and input power needed to run the thruster.

The electrospray thruster is an electrostatic thruster which uses the formation of Taylor cones to ionize the liquid fuel into droplets or molecules. The size and charge of the droplet is dictated by the mass flow rate, strength of electric field and properties of the fuel. Today's electrospray thrusters are capable of producing μN up to mN of thrust with specific impulse of 200s - 1000s. The one-dimensional calculation of thrust and specific impulse were presented to give equations of performance. Then equations were given when specific fuel choices are used in calculating the specific electrostatic calculations.

The Busek colloid thruster was designed to operate at both extremes of droplet to ions. With the ability to run in droplet mode and ionic mode by adjusting the fuel mass flow rate, the user can tailor the desired performance to the most effective method. With experimentation of the dynamic thruster, the operating window of the thruster would be optimized.

III. Methodology

In this chapter, the experimental methodology is expounded along with the laboratory equipment and the manner in which they are employed. The unique colloid thruster is further detailed. Descriptions of the vacuum chamber and support equipment are provided. The type of recorded data of the experiment is briefly detailed. The process and equipment needed in obtaining pictures of the emitter surface is explained. Finally, the error analysis is delineated.

3.1 The Vacuum Facility and Support Equipment at the Busek Company

The Busek Company allowed the author to operate the thruster first in their facilities located in Natick, MA. This set of runs demonstrated the operational capability of the thruster and the electronics package that includes the digital control interface unit (DCIU) and the power-processing unit (PPU). This testing took place in chamber number seven with vacuum pressures down to 5.5×10^{-6} torr.

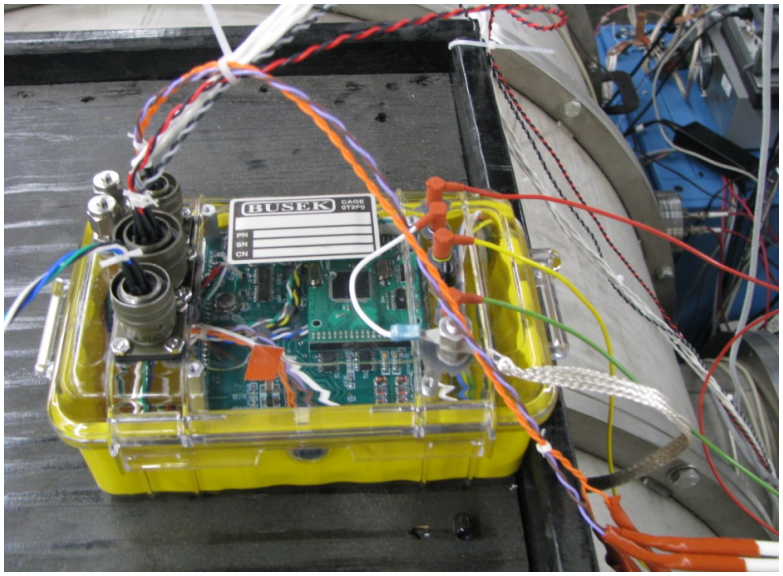

Figure 5. The electronics packaged setup for experiment

Figure 5 shows the thruster electronics package including the DCIU and PPU. For ease of testing, the thruster electronics are placed into a container that aids in the moderation of the electronics temperature. The figure also shows the computer interface cables as well as the power cables to the thruster.

The power supply units had to supply 28 volts and 5 volts to power the DCIU/PPU and communication channels respectively. These voltages are standard on space satellites. Figure 6 shows the reading of the power to the thruster. The current being displayed at that moment during the experiment was 0.156 amps and the voltage was at 28.27 volts. With power equal to the current times voltage, this thruster was operating at 4.41 Watts. This thruster when operating at max fuel flow rate will operate at around 8 Watts.

Figure 6. The DC power supply for the electrospray thruster

The thruster was placed into the vacuum chamber and the thruster electronics CPU regulated the flow of fuel to try and maintain a steady beam current. Unlike many other space thrusters, there are no visual indicators of the thruster operating visible to the

human eye. Figure 7 is a picture of the colloid thruster operating in the vacuum chamber at the Busek Company facility.

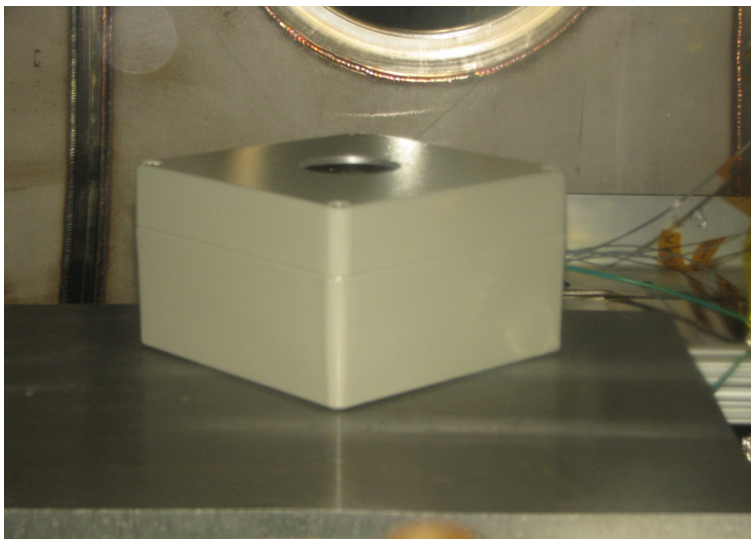

Figure 7. The colloid thruster installed in a protective box placed within the vacuum chamber

3.2 The Vacuum Facility and Support Equipment at AFIT

AFIT has several laboratories for student research. For this experiment, the Geo-orbital Nano-thruster Analysis and Testing (GNAT) Laboratory was utilized. This laboratory provided the necessary vacuum chamber for the operation and video collection for this experiment.

Located in the GNAT lab is a bell vacuum chamber capable of pressures below 10^{-8} torr . It has large front windows as well as three smaller windows at a lower location. This chamber has many feed-throughs for high voltage lines as well as BNC connections, a common type of RF connector used for the coaxial cable. Due to the small size of the chamber, the time to reach vacuum is less than 2 hours and venting operation is complete in ten minutes.

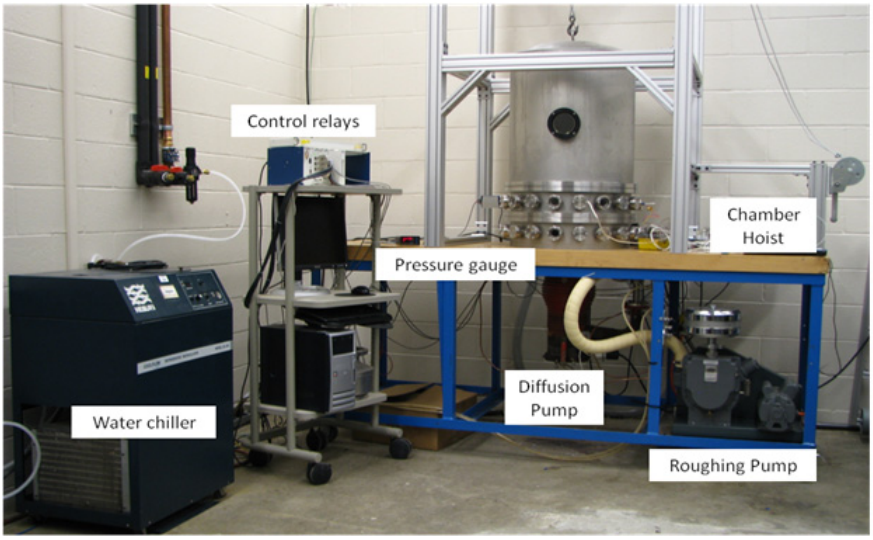

Figure 8. The Geo-orbital Nano-thruster Analysis and Testing Laboratory setup

The chamber is 0.762 meters high and 0.660 meters in diameter and uses two different pumps to obtain vacuity. The diffusion pump is a Varian VHS-6 model, and the roughing pump is a Welch 1374 belt-drive model. Figure 9 shows the diffusion pump on the left in red. There is copper tubing wound around the diffusion pump that helps in regulating the surface temperature. The roughing pump seen on the right of Figure 9 operates most of the time while the chamber is in use.

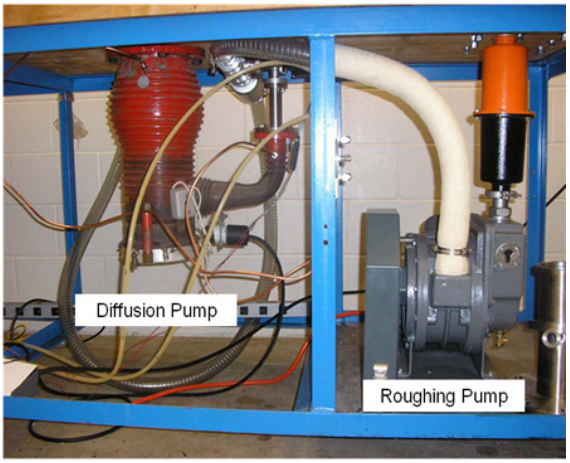

Figure 9. Diffusion pump and roughing pump

Figure 10 shows the refrigerated recirculator unit required to cool the diffusion pump before, during and just after use, or else the diffusion pump's oil vapor may enter the chamber and cover everything inside. This Cool Flow refrigerated recirculator model HX-100 is the only instrument not integrated with the computer. The user turns it on and sets the target temperature to 16 degrees Celsius. Once the refrigerator reaches this targeted temperature, the vacuum chamber is safe to be utilized. The refrigerator must not be turned off until the vacuum chamber has returned to atmospheric pressures and the diffusion pump is back to room temperatures.

Figure 10. The Cool Flow HX-100 refrigerator for diffusion pump

The chamber control computer operates the pumps and valves. Figure 11 shows the screen shot of the control computer. This program is a National Instruments LabVIEW software that, after selecting the pump down or venting, the program will automatically open and close the necessary valves and turn on and off the pumps as needed to get to the directed vacuum or atmospheric conditions. The name of the LabVIEW program file is Master. Once this file is opened, the researcher selects the

operation: pump or vent, then clicks run. With the use of this automatic program, the oil for the diffusion pump should not enter into the chamber.

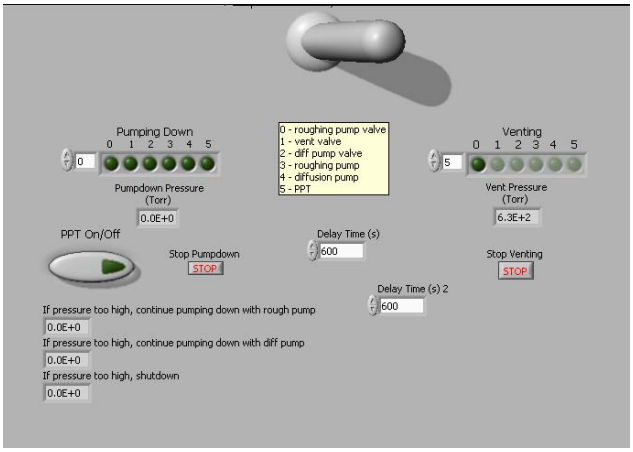

Figure 11. The vacuum chamber LabVIEW interface

The vacuum chamber uses a Terranova model 990 vacuum gauge controller that can display pressure from 4.0×10^{-10} to 8.3×10^{2} torr as measured from the Inficon BPG400 Hot Ion Combi Gauge. This pressure gauge precisely measures the analog signal from the transducer to determine pressure to within 0.1 torr. As seen in Figure 12, this reading is displayed on the unit and is also sent to the LabVIEW program to aid in the timing of operation of the chamber.

Figure 12. Pressure gage system for the vacuum chamber

When working with a vacuum chamber, the maintenance of a relatively leak-free system is required. All of the numerous connections are ensured to be properly sealed with o-rings, leak-preventing grease, and properly installed torque bolts. If a connection is improperly sealed, then the chamber will not be able to reach vacuum levels necessary to simulate a space environment.

C-clamps were installed on the chamber to secure the bell to the surface ring to squeeze the rubber gasket. This is normally not required with most experiments, but with the c-clamps use, the chamber was able to go from 5.6×10^{-6} to 6.5×10^{-9} torr. The colloid needs to operate below 1×10^{-5} torr or the high voltages will discharge into the oil plume of the thruster. The use of the c-clamps gave a greater advantage for the pumps to maintain vacuity while the colloid thruster operated at higher flow rates.

Two different power sources supplied the required power to the thruster electronics. The colloid thruster's PPU requires 28 volts with up to 9 watts of power. To supply this power the author used an HP 6266B DC power supply (Figure 13) for 0-40 volts of up to 1 Amp of the available 6 Amps. The channel was set to 28 volts using a voltmeter. An HP 62052C dual DC power supply (Figure 14) powered the communication channel. This power supply has two channels: one for 0 to 40 volts at up to 0.3 Amps and the other channel of 0-20 volts at up to .6 amps. The channel supplying the communications was set to 5 volts. This is the same setup used at the Busek Company facility.

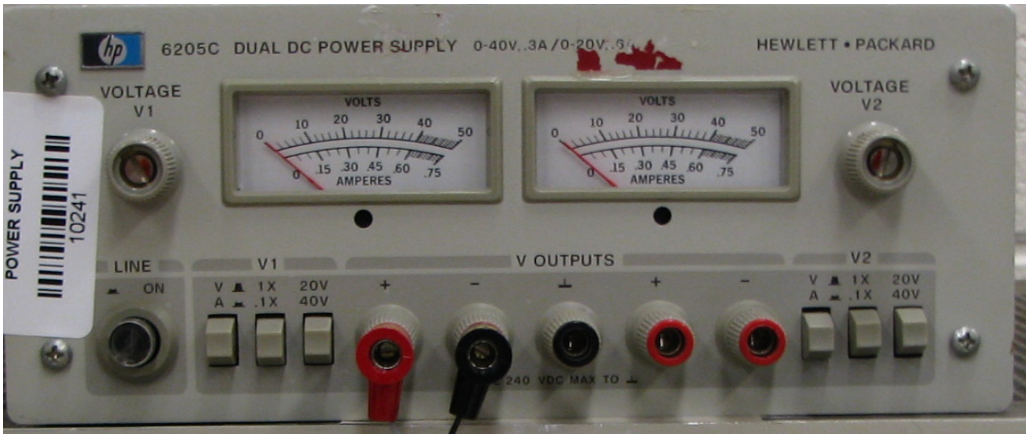

Figure 13. The HP 6205C DC power supply for communications

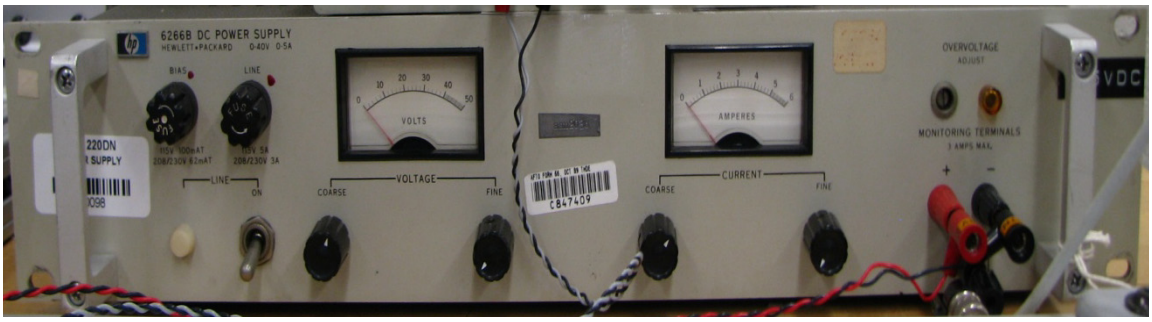

Figure 14. The HP 6266B DC power supply for the PPU

With the need to image the formations of the Taylor cones on the surface of the porous emitter, a Questar Remote Measurement System version two (QRMS-II) was employed. With this hardware the camera system can remain outside of the chamber while still being able to focus in on the droplet jets where they form. The focal length using the Questar telescope is approximately 22 inches from the front surface of the system. As seen in Figure 15, the QRMS-II is made up of floor stand, tilt head, translation stage, camera cradle, a Sony XC-77 monochrome camera, QM 1/100, QM MKIII series optics, and the computer interface to operate the system.

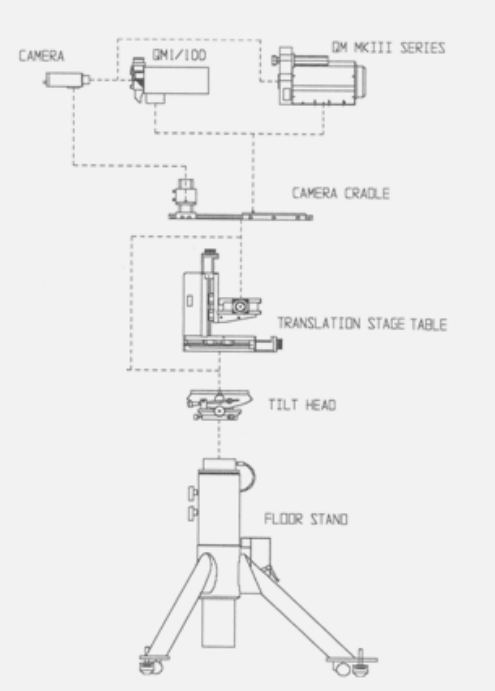

Figure 15. The QRMS-II System Assembly, taken from Questar [14]

The Sony XC-77 is a video monochrome camera module designed for the industrial market. Table 2 displays its key features [14].

Table 2. Sony XC-77 camera key specs, taken from Questar [14]

2/3-inch IT CCD camera	
Resolution	**768x493 (EIA)**
Sensitivity	**400 lux F4 (min 3 lux F1.4)**
Signal to noise ratio	**(>50 dB)**

This Questar system has a computer control to see images. The translation stage table is accurate to within .001 inches with over two-inch travel on all three axes. This allows for fine-tuning the image that is required by this magnification level. This

imaging system also has a strobe light source to illuminate the targeted object. The camera needs the light source to capture the images on the light sensor.

An aluminum thruster stand was placed within the chamber to keep the thruster in the proper orientation for the Questar QRMS-II to take pictures. As seen in Figure 16 the thruster is placed at an angle to aid in imaging the Taylor cones on the porous emitter surface of the thruster. This angle may influence the fuel to pool on one side and starve the other due to the gravitational influence interfering with the capillary effects of the porous emitter surface. But the consensus among the manufacturer, the author and his advisors was to minimize this angle while still being able to take the pictures. Further research can discover the extent of this interference by gravity on the operation of the colloid thruster.

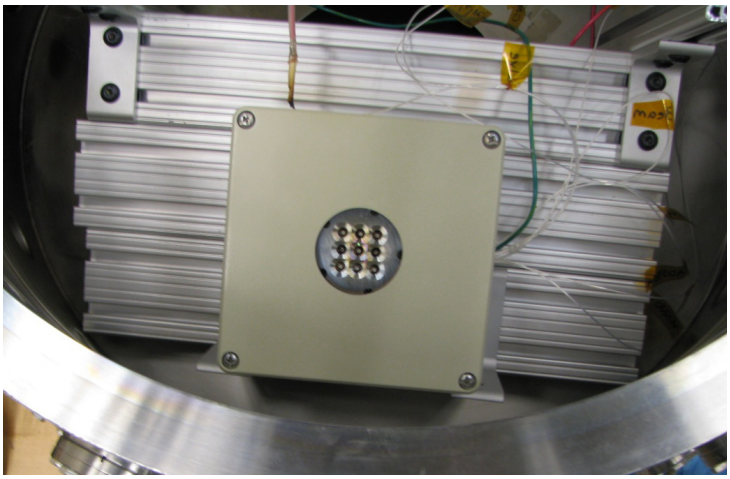

Figure 16. The electrospray thruster placed at a twenty-degree angle

3.3 The Electrospray Thruster Hardware

This section describes the electrospray thruster hardware pictured in Figure 17. These hardware pieces appear in the following order: the porous emitters, electrostatic

acceleration grid assembly, propellant storage tank, fuel flow microvalve, thruster heater and lastly the electronics package.

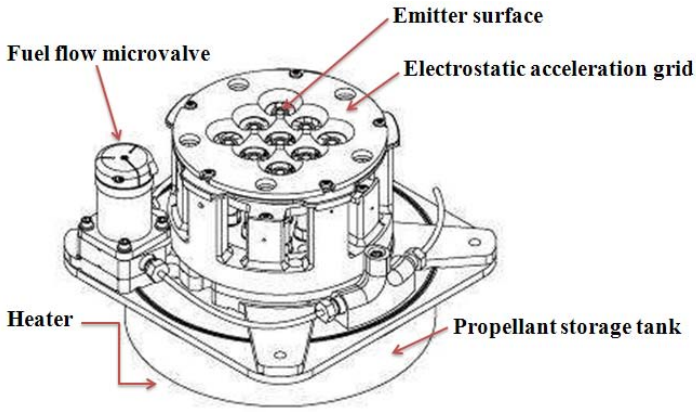

Figure 17. The key parts of the electrospray thruster, taken from Busek [1]

This prototype electrospray thruster is the first colloid thruster to use a porous emitter surface to instigate the Taylor cone formation needed to ionize the EMI Im fuel. This electrospray thruster uses Busek's ST7-DRS style thruster assembly and replaces the capillary needles with a porous emitter surface.

This type of emitter surface is a new concept and this thruster is the first hardware to demonstrate how well in reality it works as a colloid thruster. This colloid thruster has nine multiplex porous emitters to produce thrust. Instead of relying on the capillary forces to change the mass flow rate of the fuel, the Busek Company has an active control system which feeds pressurized fuel to the system by regulating flow by adjusting the supplied voltage to a microvalve plumbed in between the fuel source and the porous emitter surfaces. With all nine sites in operation, this colloid should be capable of performing up to one mN of thrust.

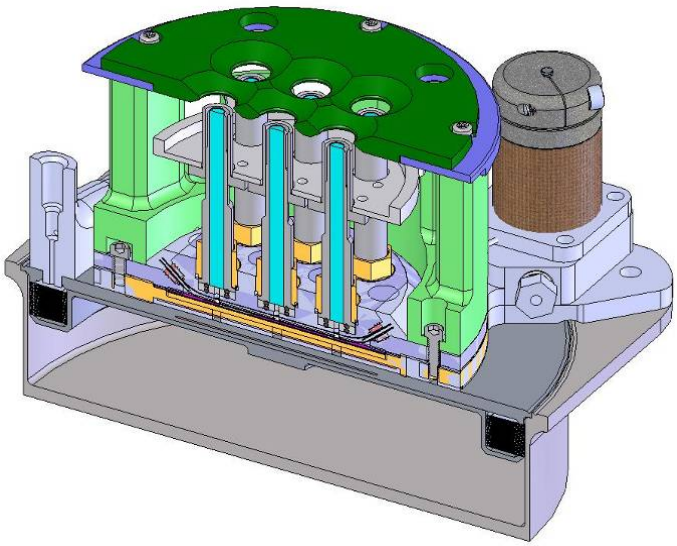

Figure 18. CAD drawing of the colloid thruster, taken from Demmons [4]

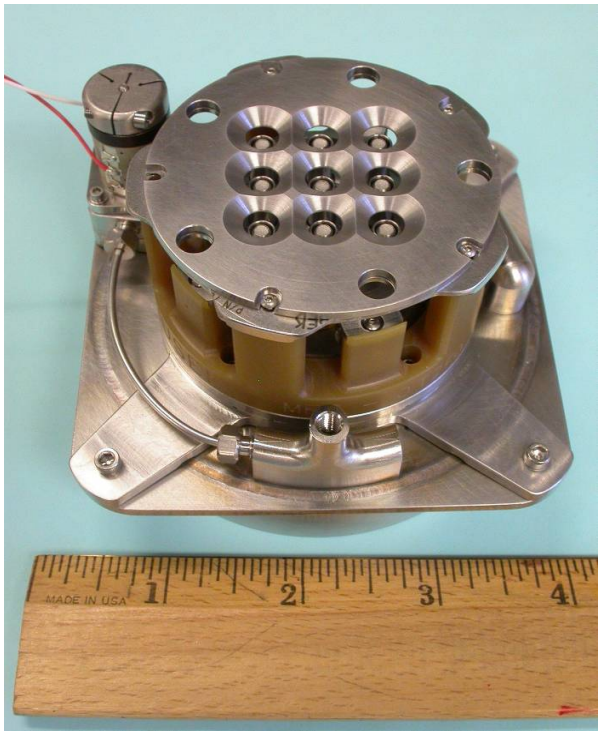

Figure 19. The electrospray thruster

The porous electrospray emitters are a unique fabricated part made of stainless steel, a material with known electrochemical issues with EMI Im. However, the stainless

steel emitters will not be damaged significantly before depletion of the 50mL propellant supplied with the colloid thruster. These specialized emitters can be reconditioned or replaced by the manufacturer, the Busek Company.

As mentioned in section II.6, the use of the porous emitter allows the thruster to operate at a greater thrust range compared to traditional colloid thrusters. With this surface the number and formation location varies with the flow rate of the ionic fluid. To accomplish these formations effectively the Busek Company has developed a proprietary porous surface shape that enables electrospray emission across the entire surface. This shape is patterned after the uniform electrostatic field across the entire surface, allowing for emitted droplets of approximately the same charge-to-mass ratio from the entire surface. As seen in Figure 20 the rough surface is the porous stainless steel.

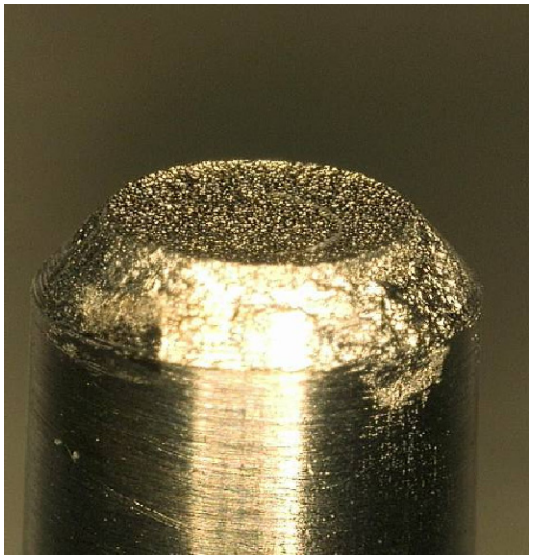

Figure 20. The porous stainless steel emitter with a parabolic surface, taken from Demmons [4]

Due to manufacturing limitations, the final emitter is not ideally matched to the electric field. The center of the emitter is slightly more distant from the electric field

compared to the rest of the surface shape, which allows pooling to occur in the center before the outer circumference becomes saturated. This anomaly may be captured using the specialized imaging equipment.

The next key hardware item discussed is the electrostatic acceleration grid. The extraction grid assembly maintains high electrical impedance between the beam and extractor for thousands of hours of operation. The entire extraction grid assembly is removable for ease of thruster cleaning and maintenance. The PPU supplies -1 kV to this acceleration grid. This is critical in the operation of the thruster. Between the beam and the extraction grid is a 10 kV differential used in accelerating the ionic droplets for thrust. In Figure 21, the black arrow points to the acceleration grid plat, and the red arrow points to the void within the holes for the formation of the electrical field.

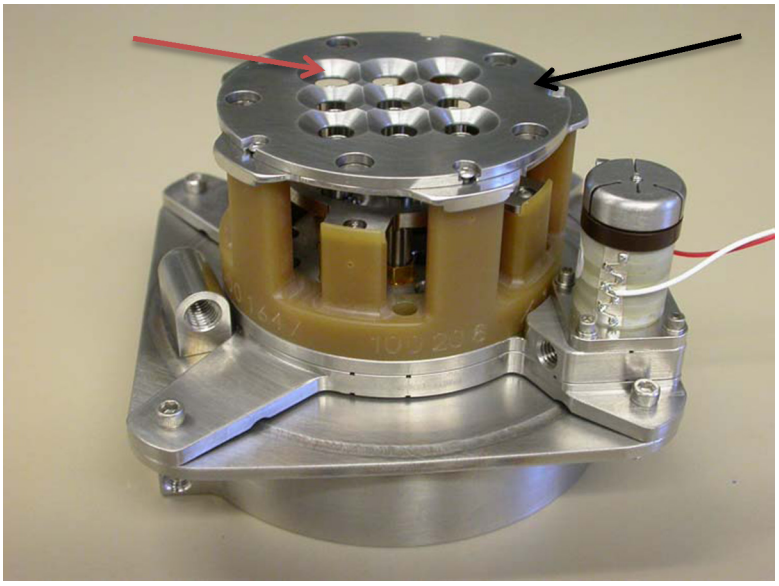

Figure 21. The round ring from the drilled holes is the acceleration grid, taken from Busek [1]

The propellant storage tank is the next hardware item presented (Figure 22). The liquid propellant is stored in a 50mL metal bellows pressurized to 30psi with dry and

filtered nitrogen. The use of this inert gas is for short term testing, as the volume around the outside of the bellows will not change significantly, resulting in minimal loss of drive pressure. For operations lasting longer than 100 hours, the tank should be permanently connected to an external pressure source or filled with a vapor pressure liquid, such as butane, to maintain pressure. The propellant storage tank is pressurized at all times, which significantly reduces the possibility of gas penetration into the feed system.

Figure 22. The propellant tank bellows before it was welded together, taken from Demmons [4]

The most important piece of hardware for this thruster is the fuel flow microvalve. The colloid piezo-actuated microvalve regulates propellant flow to the emitter (Figure 23). The microvalve actuation voltage is 0V to 200V. The microvalve has a small actuation stroke that allows the pressurized fuel to flow past. The thruster's electronics regulates the voltage to the valve to obtain the desired propulsion. The movement of the piezo-actuated microvalve is linear but the actual fuel flow rates are nonlinear. This flow rate is a function of the pressure found within the fuel tank, the amount the valve is open, the resistance and capillary affect of flow through the porous emitter.

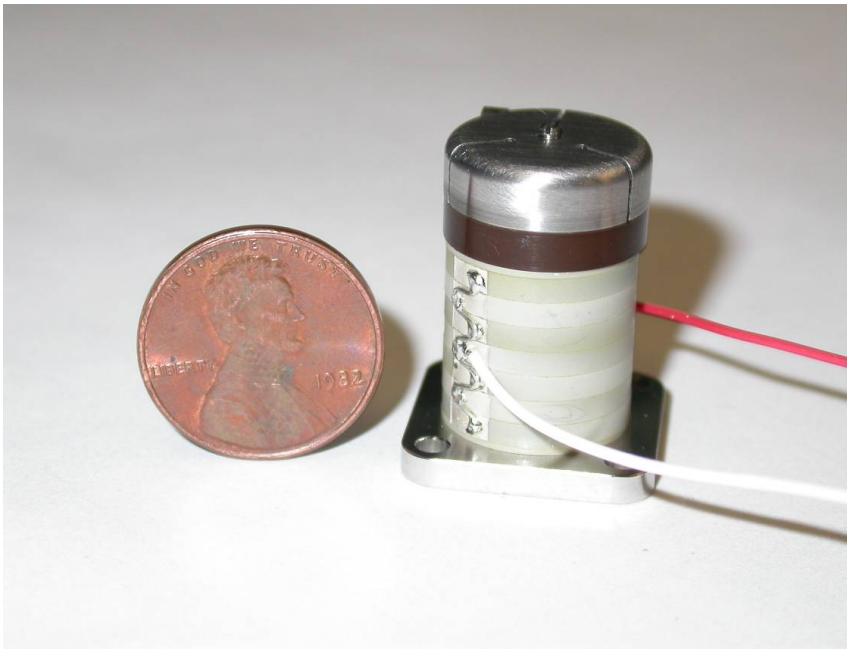

Figure 23. The propellant flow microvalve, taken from Busek [1]

When the thruster is operating, the voltage of the fuel microvalve is commanded to reach a desired level and the CPU within the electronics package ramps up the voltage slowly because the resultant fuel flow through the emitter is nonlinear. If the thruster electronics detects a short out condition or other anomalies, the microvalve closes automatically. When the microvalve closes after allowing fuel through, the fuel lines still maintain some residual pressure within them. The pressurized ionic fluid within the fuel lines continues to flow though the emitter until this pressure equalizes with the natural resistance to this flow, due to the porous surface.

The piezo-actuated microvalve is sensitive to mechanical shock due to its small size and stroke. A direct impact or high shock may cause the valve to leak or fail to open. Also, when the thruster system is going into prolonged storage, the pressure of the propellant storage tank should be reduced to 1psi, which decreases the stresses on the microvalve.

At the bottom of the thruster is the heater. This thruster was built with all needed features for operating in space; including a heater mounted inside the thruster enclosure to maintain thruster temperature (Figure 24). The heater is a high wattage resistor with a temperature sensor incased in a polyimide cup using a urethane-potting compound. The heater can operate to 15 watts of power. On the right side of Figure 24, the white material is a thermal interface placed over the heater to improve thermal conduction between the heater and the underside of the thruster's propellant bellows.

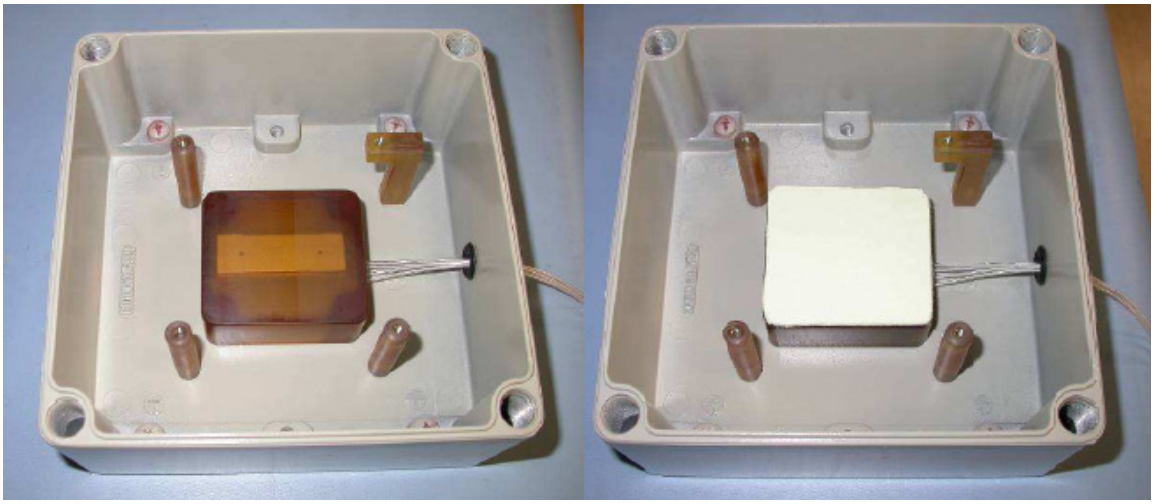

Figure 24. The thruster's heater without/with thermal interface added, taken from Busek [1]

3.4 The Electrospray Thruster Electrical System

The electronics package for this colloid thruster includes two major parts: the digital control interface unit (DCIU) and the power-processing unit (PPU) and is physically broken down to: (1) the digital control interface unit (DCIU) board, (2) the housekeeping board and (3) the HV board.

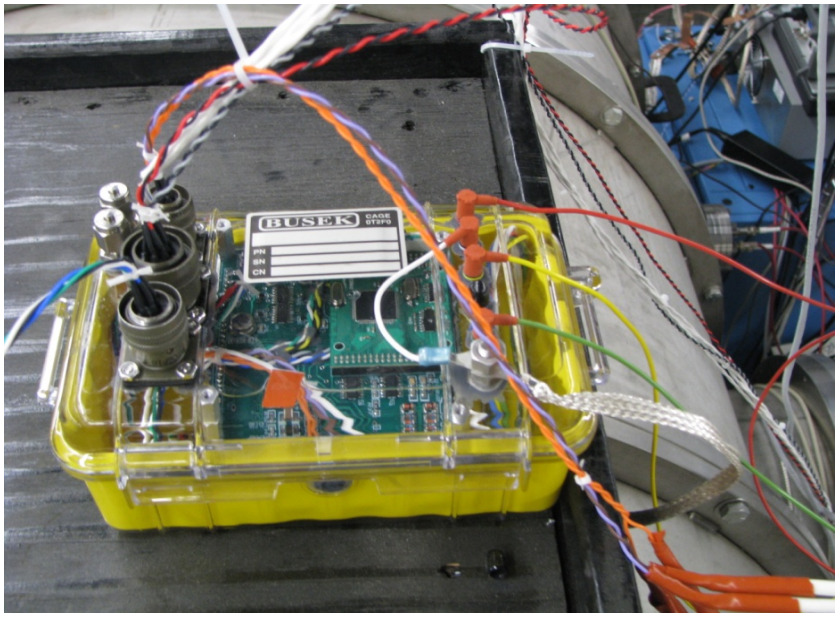

Figure 25. The electronics package for the colloid thruster

With this DCIU/PPU system designed for operating on a CubeSat, there are a few unique features. The combined electronics is sized for 10 cm by 10 cm by 4 cm and is seen in Figure 25. For ease of use and repairs, the electronics houses within a container filled with Flourinert electronic liquid developed by 3M. Flourinert is a specialized liquid that electrically insulates and is used in various cooling applications. With this type of packaging, the electronics cannot be placed within the chamber for testing.

With this colloid thruster capable of one mN of thrust, the emitted currents pushed beyond 100μA. The PPU needs to provide the capability for neutralization and the electronics be isolated from the spacecraft ground. Previous needle design colloids could emit no more than 5μA per thruster, making a cathode irrelevant because photoemission from the spacecraft's solar panels would provide sufficient emitted negative current to keep the spacecraft from charging.

Table 3. Complete list of command and telemetry for DCIU/PPU, data from Busek [1]

CHANNEL 16 BIT RESOLUTION MONITORS:	Maximum Value	Units
BEAM OUTPUT VOLTAGE	10	kV
BEAM OUTPUT CURRENT	0.5	mA
VALVE OUTPUT VOLTAGE	200	V
EXTRACTOR OUTPUT VOLTAGE	-1	kV
EXTRACTOR OUTPUT CURRENT	100	uA
CNTC OUTPUT VOLTAGE	-800	V
CNTC OUTPUT CURRENT	1	mA
TCOM FLOAT VOLTAGE	50	V
10 BIT RESOLUTION MONITORS:		
SYSTEM TEMPERATURE	150	C
HEATER TEMPERATURE	150	C
HOUSEKEEPING + SUPPLY VOLTAGE	15	V
HOUSEKEEPING- SUPPLY VOLTAGE	-15	V
SYSTEM INPUT CURRENT	350	mA
10 BIT RESOLUTION COMMANDS:		
BEAM OUTPUT VOLTAGE	10	kV
VALVE OUTPUT VOLTAGE	200	V
EXTRACTOR OUTPUT VOLTAGE	-1	kV
CNTC OUTPUT VOLTAGE	-800	V
HEATER OUTPUT POWER	2	W

The first major part of the electronic package is the digital control interface unit (DCIU). This DCIU enables communication between the host computer running LabVIEW and the thruster electronics using a standard RS-422 communication protocol. The power converters commanded by the DCIU operate the thruster. The resulting telemetry is then sent to the DCIU and correspondingly is sent to the host computer. The complete list of the available telemetry is presented in Table 3.

Within the DCIU is the Housekeeping Board containing the power bus conditioning and the isolated power converters for the processor and monitoring circuitry. The PPU operates off a 24-36VDC bus voltage nominally set for 28 Volts. The power input is isolated from the chassis for the operation of the carbon nanotube cathode independently from the main bus reference. The auxiliary voltages required within the electronics are ±12V and +5.2V.

The power-processing unit (PPU) utilizes highly efficient high voltage (HV) converters to operate the beam, extractor, and cathode electrodes. Each of these HV converters has current and voltage monitors to provide telemetry to the DCIU and are accurate to within 1%, and operate with <0.5% voltage ripple. The DCIU uses this telemetry to insure the health of the power conversion system and the operation of the thruster. The valve converter is also located on the HV board and is referenced to the beam potential. The beam electrode is designed to handle up to 10 kV while the extractor is designed to operate voltages of -1 kV. The outputs of converters are independently and linearly controllable via the DCIU.

Table 4. Ratings for the regulated DC power converters, taken from Busek [1]

Type of converter	Maximum Voltage	Maximum Current
Heater	50 Volts	1 A
Beam	10,000 Volts	600 uA
Extractor	1,000 Volts	1mA
Cathode	800 Volts	1.2 mA
Valve	200 Volts	

The digital control interface unit (DCIU) for the electrospray thruster contains a small central processing unit (CPU). This CPU board contains a processor, memory,

analog to digital conversion, and real time clock. The processor contains firmware comprised of algorithms that handle tasks from communication to implementing the control loops required to maintain the thruster's operating set point.

The software code is broken into four main tasks: (1) maintain closed loop control of the thruster, (2) receive and decode commands from the host simulator computer, (3) update system set points according to commands, and (4) protect and report the thruster's system health and status telemetry. The processor has three operating modes. The nominal operation mode commands are made to maintain a steady thrust output level. In this mode, the CPU regulates the fuel flow micro-switch to maintain the calculated thrust. This has not been fully optimized or calibrated. The beam command mode regulates the voltage and current separately. The final mode is the manual command mode. This mode allows the user to modify every settable system value and may be used to debug the CPU system.

3.5 LabVIEW Interface

The executable program supplied was written using LabVIEW 8.6. Operations between the computer and the thruster electronics are asynchronous. This means the DCIU/PPU will continue operating with respect to all previous setpoints and commands with its built-in programming. As the commands and setpoints are updated, using the serial interface, the onboard CPU then uses these new parameters to adjust the operation of the thruster. The executable commands are constructed and sent based on event structures initiated by user events.

There are three preprogrammed thruster operational modes: manual, beam current control, and thrust control. Manual mode should only be used for voltage checkouts when looking for beam and extractor leakage currents. Mode independent command variables include beam and extractor voltage.

Beam current control mode allows for a specific beam current to be maintained, which is adjusted by modulating propellant flow to the thruster. This is the preferred method of operating the thruster. The selection of this mode is required when the thruster is first operated, because there is a 1 to 2 hour delay from when the propellant valve is first opened and emission is obtained from the thruster. If the user operated the thruster in the beginning with the other two modes, the thruster may easily become flooded causing the thruster to short out.

Thrust command mode is similar to beam current control mode, but instead of entering a beam current, the user commands the desired thrust. The beam current required to achieve the commanded thrust is used as a control point. This mode of operation is not fully exploitable until the thruster thrust has been fully calibrated. This mode would be the desired mode to be used in space maneuvers. Currently a rough mathematical model calculated the thrust and is not calibrated to actual thrust produced from a colloid thruster.

Currently, to achieve electrospray emission, the beam voltage should be set to 9kV and the extractor voltage to -1kV. With these settings, the electronics of the thruster adjusts the thrust output by regulating the fuel flow through the porous emitter surface. With future tests involving the thruster's operation at different beam voltages, the region of stable emission should be found. A major reason for modulating the beam voltage is

that this is another method for varying thrust. With future work, more complex algorithms will be developed which may include adjusting beam voltage and current for optimum thruster performance.

Another item manipulated through the interface is the cathode. A carbon nanotube field emission cathode was supplied with the colloid thruster system. This cathode would be required for beam neutralization and spacecraft charge balancing in a flight system. The cathode can be manually commanded to voltage up to -800V, resulting in electron currents in excess of 1mA. The cathode can also be operated in a closed loop control mode, where the cathode attempts to balance the emitted charge by monitoring the float voltage of the PPU.

The continued cathode operation in confined vacuum tanks leads to cathode contamination. With the colloid operating within a chamber, the backscatter from the colloid beam hitting the tank wall and the buildup of fuel in the chamber lead to the contamination. The cathode was packaged separately so that it can be placed in the tank only when testing requires it and was not used for this experimentation.

To keep track of all the telemetry, the author used the graphical display interface (Figure 26). The LabVIEW display has digital readouts of all thruster and housekeeping data presented within a tab selection on the left hand side of the control panel. In addition, two graphs are presented on the right hand side of the screen. The choice of which telemetry to display can be selected from drop-down menus above the graphs. The telemetry choices include time, beam voltage, beam current, extractor voltage, extractor current to name a few. This allows the user to observe channels of interest while the experiment is progressing and all data is recorded for further analysis.

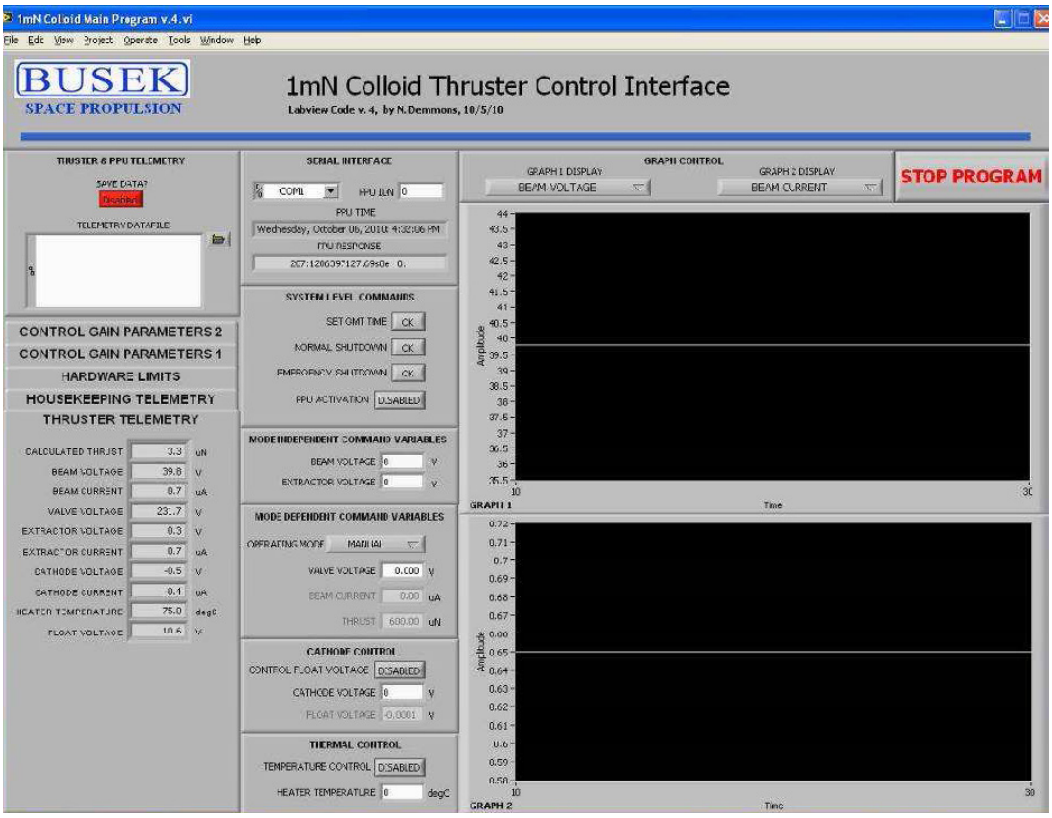

Figure 26. Screen shot of the LabVIEW display

3.6 Experiments to Meet Thesis Objectives

The experiments were developed to meet the thesis's four objectives mentioned in section 1.5. First, give AFIT a working colloid thruster in its vacuum chamber labs. Second, ensure that the colloid thruster is operating properly. Third, capture the flow patterns of this thruster, from the droplet domain to ion domain. Fourth, explore the operating envelope of this specific thruster and measure its performance.

The following portion of this paper includes the experiment that meets the first objective of giving AFIT a working colloid thruster in its vacuum chamber labs. This experiment normally takes place as a subset of all other experiments. However, because this prototype hardware could only be operated on a site visit to the Busek Company in

the early stages of the research, it seemed prudent to perform this experiment on its own. A more detailed description of many of these steps can be found in the thruster's operation manual. Some of these setup steps are for follow-on experiments.

The basic steps follow. Build a stand that can safely hold the thruster in the vacuum chamber. This is required due to the hole in the bottom of the chamber for the diffusion pump. The stand is made out of an aluminum 80/20tm commonly found at AFIT. Place the stand into the chamber and tilt the stand in such a way that images may be taken of the thruster surface through a port hole while the thruster operates is in operation. The final tilt of the thruster resting on the stand is roughly twenty degrees.

Following the instructions found in the thruster manual, the thruster was wired into the chamber with all electrical wires connected with their electrical pass-through. Outside the chamber the DCIU/PPU was wired to the corresponding pass-through of the chamber. Thus, the electrical system was wired for operation. The DCIU/PPU was then connected to the power sources and to the computer while all rested in unpowered states.

The author then pumped down the chamber using the corresponding LabVIEW program ensuring the final equilibrium pressure was below 1E-5 torr. After waiting for over 48 hours, the specified time in the manual, the thruster was tested for any short circuits. This was done by applying 28 volts and 5 volts of DC power to the PPU. Then, opening the thruster corresponding LabVIEW interface, the experiment started with all command variables set to zero volts, and the com-channel set to the appropriate selection. The PPU activation button was enabled and a data log file created and set to record.

With the telemetry streaming to the LabVIEW, the control interface operated appropriately. Next, the manual command mode was used to adjust the beam voltage to

10 kV in 250 V intervals. After the beam reached 10 kV, the extractor was then commanded to 1 kV (the interface is programmed to display only positive numbers in the command window).

Detecting a short circuit, demonstrated by the current of the beam or extractor reading climbing extremely high or the sounds and smells of arcs formations, the operator set the power back to zero. With the power supplies cut, the communication to the LabVIEW interface terminated. This means there was a short in the system. The wires needed to be checked and the short fixed. The process was repeated until the desired full power beam reached 10 kV, and the extractor reached 1 kV with little or no leakage of current.

The Busek Company stated that the operating voltage of the thruster, 9 kV for the beam and 1 kV for the extractor, was set using the computer interface. The computer used the closed loop beam current control, set to 20 μA, to change parameters for the thruster operation. This closed loop beam current control setting allowed the electronics CPU to adjust the voltage to the microvalve switch in regulating the flow of fuel through the porous emitter to try and maintain the set current. This permitted the electronics to fill the fuel lines without flooding the surface and causing impingement on the surface of the emitter. This setting also helped to clear bubbles that formed on the inner surface of the fuel lines. The thruster operated for over eight hours initially with this setting. According to the manufacturer, at this point the thruster should be ideally primed to operate with a beam current ranging from 0 μA to 300 μA.

The following portion presents the experiment for the second objective, ensure that the colloid thruster is operating properly. The thruster operation was tested at the

Busek Company and at AFIT. This allowed the reliability of the thruster to be confirmed before delivery and ensured that data comparison could be performed to guarantee the thruster operation. The comparison is limited to the thruster operating under a closed loop beam current setting of up to 40 μA. This limitation is due to the loss of vacuity with any higher flows in the Busek Company vacuum chamber.

Also to meet this objective, the electronic interfaces were set to monitor the electrical system for discharges in the plume and impingement on the surface of the thruster. LabVIEW would then alert the user with error codes and an impingement light. If the problem threatened the long life of the thruster, the onboard CPU would command the shutdown of the thruster without user input.

In addition, to test the operation of the thruster, the thruster was manipulated to beam current values of up to 300 μA. The operating thruster also tested the bell chamber capability to hold vacuity. This was done by setting the beam current to the maximum value; this corresponds to the highest flow of charged EMI Im expelled into the chamber.

The next experiment addressed objective three, capture images of Taylor cone formations. This experiment was to use the Questar's QRMS-II camera system to capture the Taylor cone formations with the thruster operating at different beam current values. This required the setup of the QRMS-II outside of the chamber with the stand tilted, allowing the camera to see the thruster features of interest through the small chamber portholes. Since this system had not been used for a few years, the author had to rediscover the practical knowledge for operating the system beyond what was provided by the user manual.

First stage was getting the camera system up and running. The QRMS-II was assembled according to the user manual and powered up. The computer interface had to be learned and fined tuned. Several black and white camera target images were printed on normal office paper; this allowed the camera to focus on an easy target. Much trial and error revealed that the focal length while using the long lens was 22 inches. From this distance, the camera would show individual ink droplets on the target paper, and would only be in rough focus on the monitor for 0.075 inches. This distance is in the direction of the target paper. See Figure 27.

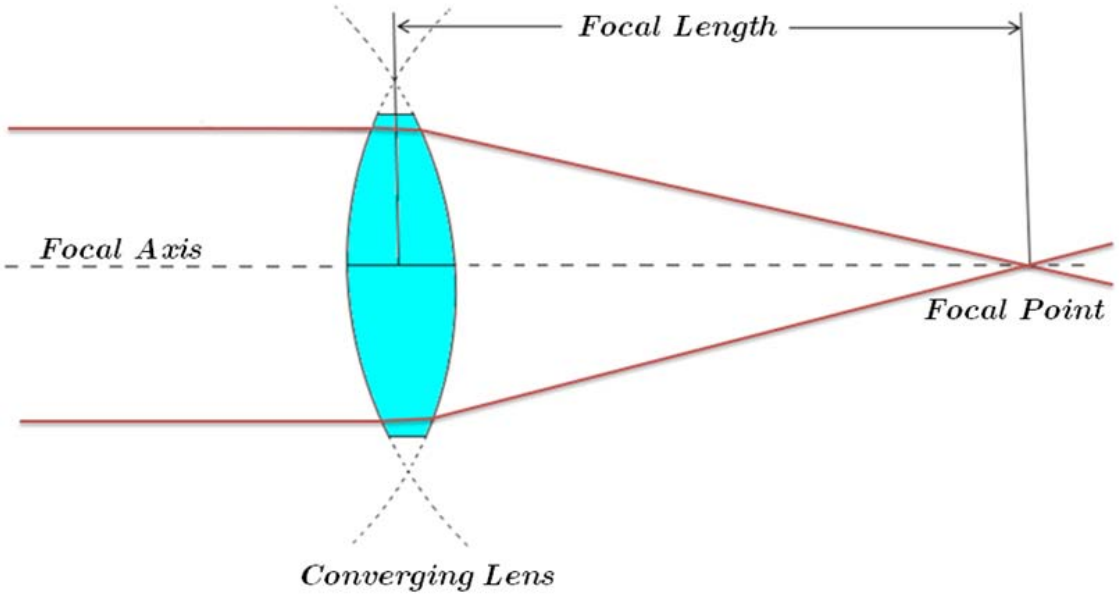

Figure 27. The focal point with a converging lens

With time, the user discovered that with the light source turned on and focused on a sheet of paper, the overall stand should be placed roughly twenty-two inches from the target and the set screws holding the camera in place should be loosed so that it could slide to the point where the focused light was the smallest. Figure 28 highlights the set

screws for the focusing of the light on the target. Under- and over-focused light is larger in diameter and dims, as the light is de-concentrated.

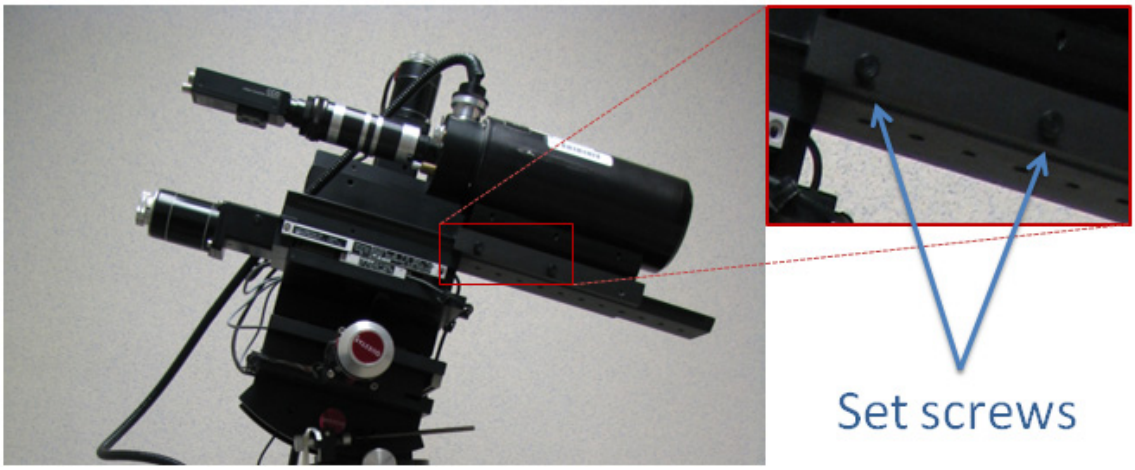

Figure 28. These set screws aid in the focus of the camera system

With this knowledge, and with the understanding of the use of the available filters controlled by the computer interface, the user next aligned the camera to the thruster. With the camera tilted in a downward angle and the thruster situated at twenty degrees, the camera had a clear view of the porous emitter.

The last objective was to measure the performance of the thruster within the full operation envelope. The most important performance characteristic to capture was the electrospray colloid thruster's produced thrust. The torsional thrust balance (Figure 29) is a stand that uses a calibrated capacitive force generator to measure the thrust down to the μN. The thruster is traditionally installed with the thruster firing horizontally on the balanced control arm with a counterweight placed on the opposite side. As seen in Figure 30, there are two electrically charged plates acting as parallel plate capacitors.

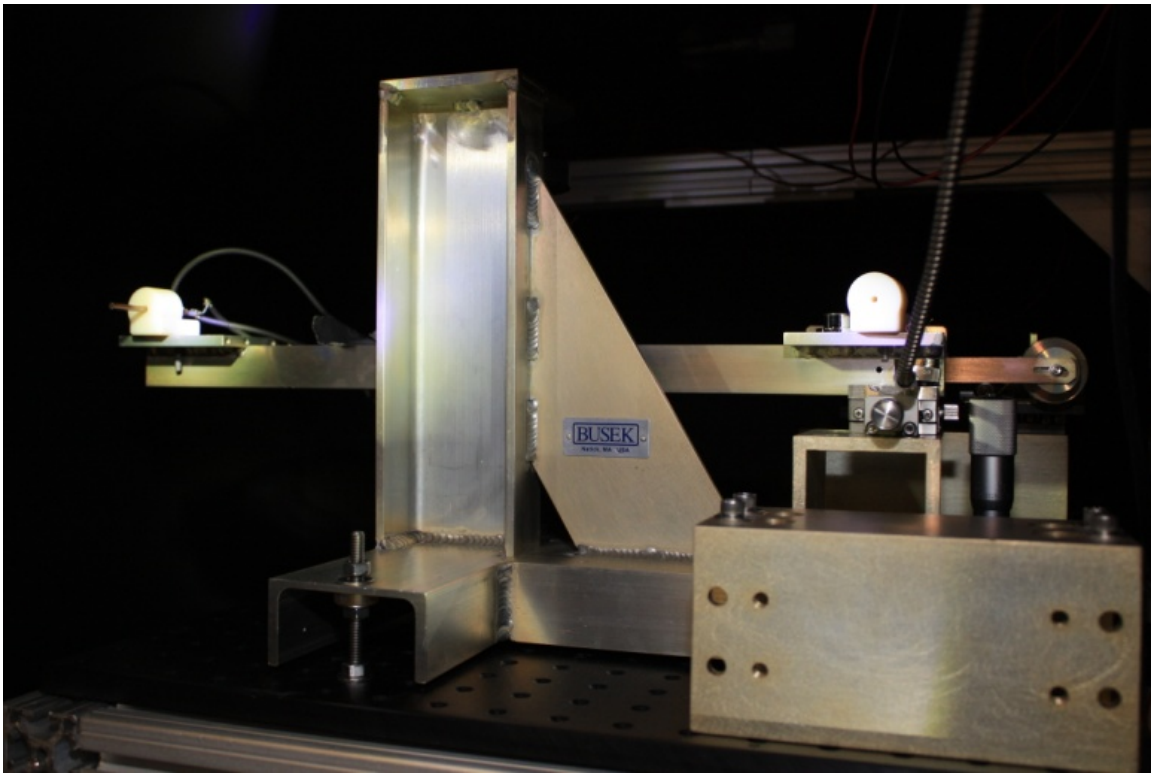

Figure 29. The Busek torsional thrust balance for electric thrusters

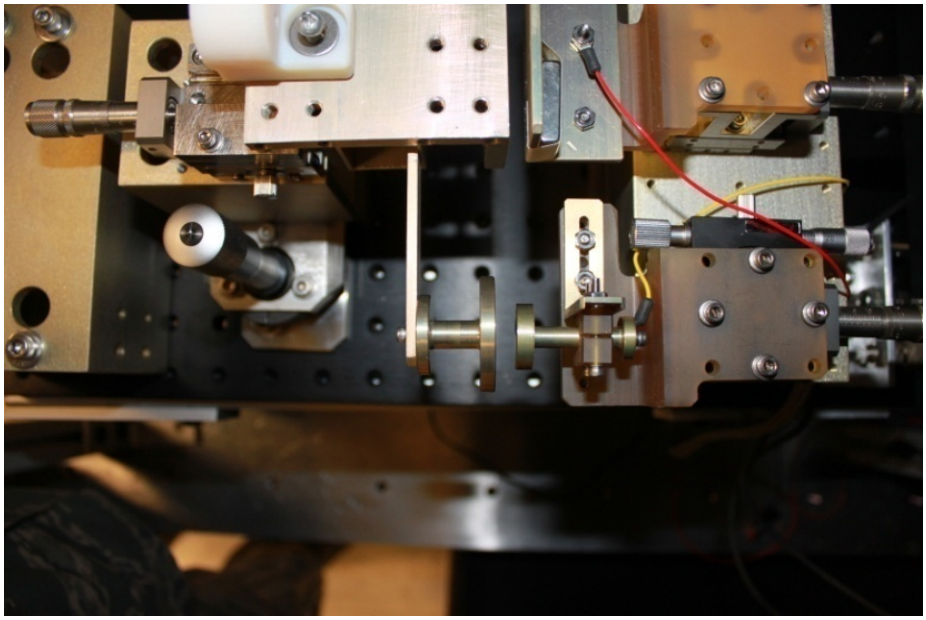

Figure 30. The parallel plate capacitors of the torsional balance

Having an equation for the charge and electric field for each plate, a relationship for the force, F, between the plates can be found, knowing that the force is equal to the charge on one plate multiplied by the electric field from the other. In the torsional balance setup, the two plates act as parallel plate capacitors.

With the torsional thrust balance, a calibration run is used to find the ratio of μN/V. This ratio corresponds to the voltage required to keep the distance between the electrodes constant while the thruster in running. The measured voltage then is used to discover the corresponding thrust.

Under the Busek Company's direction, the thruster operation generally took place in the vertical direction. The effects of gravity on the porous emitter surface at various flow rates could interfere in the fine balance of Taylor cone formations and cause excessive impingement. To overcome this, the author theorized that the thruster could be installed in the twenty degrees off vertical orientation on the thrust balance. Then using trigonometry, the thrust of the thruster could be calculated assuming that the thrust in the vertical direction will not overwhelm the corresponding horizontal calculation.

3.7 Error Analysis

Data collected in analysis were subject to various errors. These errors include three major categories: precision, bias and accuracy. In order to account for the total error, error bars are usually included on critical graphs. When performing statistical experimentation, the error would be determined from equation 15, using the accuracy of the equipment used to collect the data (θ), the standard deviation (σ), the number of data points captured (n) and the bias (b). Where t is selected by the required confidence

factor. As a general rule, if an error from a particular source is significantly smaller than the other errors present, it is not to be used in equation 15.

$$error = \sqrt{\left(\frac{t\sigma}{\sqrt{n}}\right)^2 + (\theta^2) + (b^2)} \qquad \text{Eq. 15}$$

According to Hill and Chang the calculation of these errors can get quite complex. The normal probability distribution, curve-fitting samples from a normal population and least-square curve fits may be required in calculating this precision error [11].

Typically, the instrument manufacturers quoted accuracy for their instrument include errors from all sources. With all data being recorded by the thruster electronics package, the total error for these experiments are only determined by the accuracy and resolution of the sensors used in recording the telemetry. According to the operating manual for this thruster, each of the converters has output voltage and current monitor circuits. The outputs are accurate to within 1 percent of the reading, while the resolution is far greater in all channels. All graphs developed from this data would then have an error bar that goes 1 percent above and below the telemetry readings. With the error being at a constant percentage on all telemetry, the error bars will not be presented in any plot. The information supplied by the manufacturer and the maximum values of the channels can be seen in Table 5.

Table 5. Complete list of minimum accuracy for the telemetry from the DCIU/PPU, taken from Busek [1]

CHANNEL 16 BIT RESOLUTION MONITORS:	Maximum Value	Units	Output Accuracy within	Units
BEAM OUTPUT VOLTAGE	10	kV	100	V
BEAM OUTPUT CURRENT	0.5	mA	5	μA
VALVE OUTPUT VOLTAGE	200	V	2	V
EXTRACTOR OUTPUT VOLTAGE	-1	kV	10	V
EXTRACTOR OUTPUT CURRENT	100	uA	1	uA
CNTC OUTPUT VOLTAGE	-800	V	8	V
CNTC OUTPUT CURRENT	1	mA	10	μA
TCOM FLOAT VOLTAGE	50	V	500	mV
10 BIT RESOLUTION MONITORS:				
SYSTEM TEMPERATURE	150	˚C	1.5	˚C
HEATER TEMPERATURE	150	˚C	1.5	˚C
HOUSEKEEPING+ SUPPLY VOLTAGE	15	V	150	mV
HOUSEKEEPING- SUPPLY VOLTAGE	-15	V	150	mV
SYSTEM INPUT CURRENT	350	mA	3.5	mA
10 BIT RESOLUTION COMMANDS:				
BEAM OUTPUT VOLTAGE	10	kV	100	V
VALVE OUTPUT VOLTAGE	200	V	2	V
EXTRACTOR OUTPUT VOLTAGE	-1	kV	10	V
CNTC OUTPUT VOLTAGE	-800	V	8	V

In summary, this chapter presented the facilities, hardware and key computer interfaces that were required to complete all experimentation. The Busek electrospray thruster was covered in great detail. Operation of this prototype thruster at AFIT would be a huge step forward. To meet the thesis objectives four experiments were also presented.

IV. Results and Analysis

This chapter is broken down into the three parts of the experiments to meet the first three thesis objectives. Within each of these three sections will be the recorded results and analysis. These sections also contain the obstacles and some solutions to the experimentation. The experimentation for the fourth objective was not completed by the end of the allotted time and will not be presented in this chapter.

4.1 Operating the Thruster at AFIT

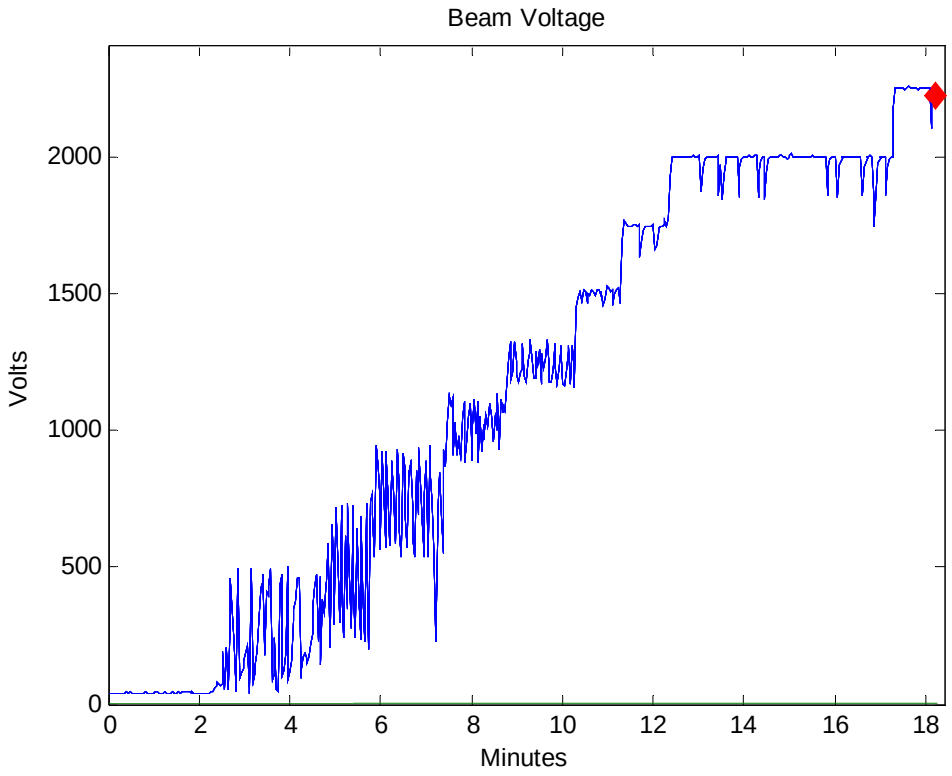

Figure 31. The test for short circuit condition, red star represents short out

The initial operation of the thruster went through a short circuit test to ensure there were no short circuits in the wiring to the thruster or within the thruster itself. Following

the procedure from 3.6, the first ramp up of the beam voltage shorted out at 2,250 volts (see Figure 31). The blue line shows the recorded beam voltage over time with sampling rate close to every second. The red star represents the short out condition point. Upon investigation, the BNC connection for the piezo-actuated microvalve shorted out with the connection to the alligator clip. This line should only carry a maximum of two hundred volts and at this stage have no power at all, yet it shorted out when the beam voltage reached 2,250 volts.

The evidence that the beam shorted out was a jump of the beam current to 637 µA while the current of the extractor remained constant. A power spike was accompanied by a high-pitched whine and scent of ozone. The amperage on the power supply spiked to over 1 A. This was a potentially risky state, so the user immediately turned off the power supply. When the power supply was turned back on and a voltage of 250 volts was applied to the beam, the beam current jumped from 7 µA to 150 µA, so the user cut the power right away and rewired the package.

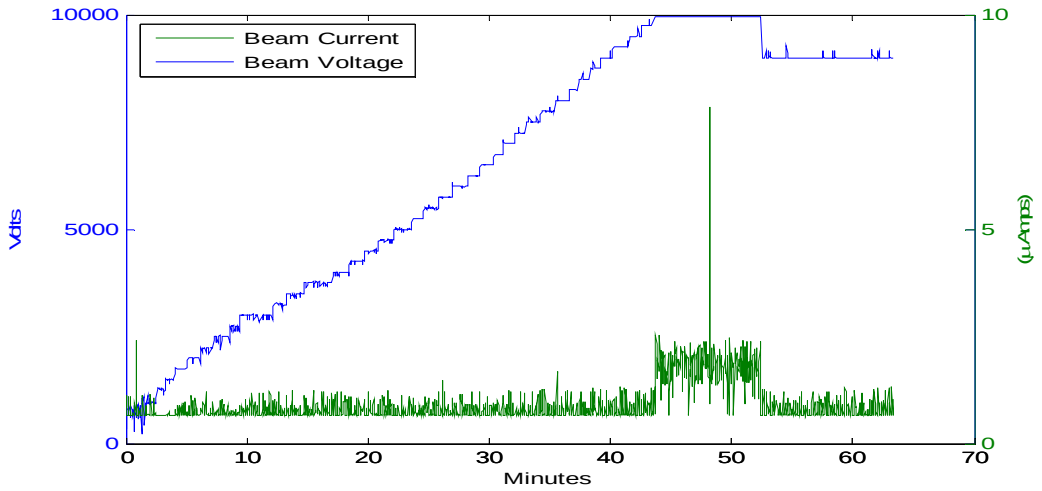

Figure 32. The beam voltage and current readings on final short circuit test

Once the rewiring was completed and the switch went through a high power pass-through, the beam shorted out at 4,000 volts. At this point the user wired the beam through a high power pass-through as well. With this done the beam voltage was able to obtain 10 kV, the blue line in Figure 32. At this voltage, the current bleed went from hovering around 1.0 µA to 2.3 µA with a spike of 7 µA, the green line in the figure. That spike represents the moment when the extractor voltage was set to -1 kV.

The author monitored the voltage step-up for the short circuit test at the same time as monitoring the current to the beam and the extractor. Figure 33 shows these readings. The blue line represents the same beam current as the green line in Figure 32. The red line represents the extractor current. At around the 45-minute mark when the beam voltage was at the maximum setting of 10 kV, the extractor current also climbed from base state. With the extractor and the beam currents above baseline at beam set to 10 kV,

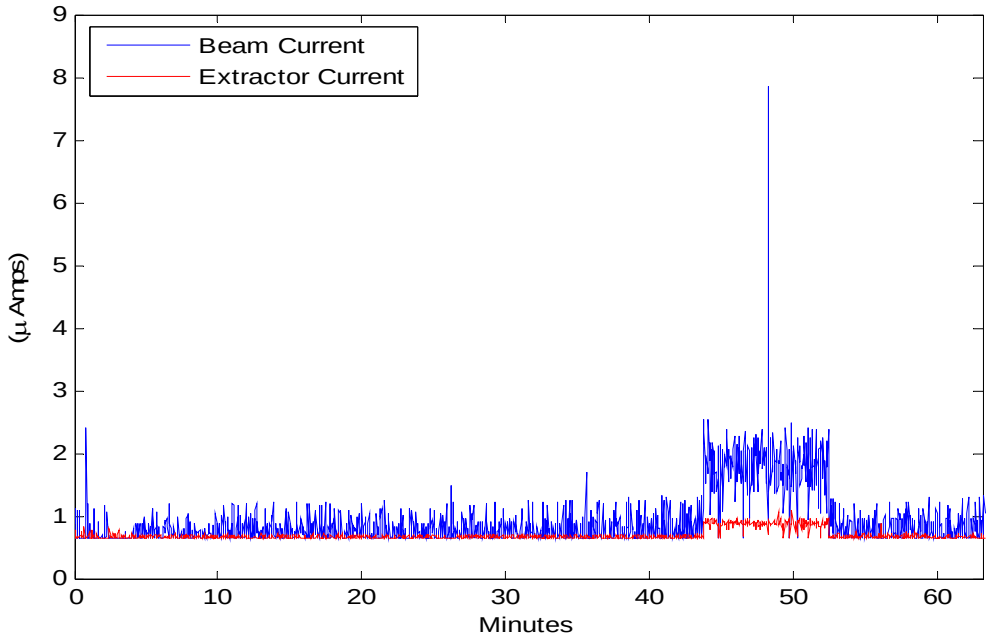

Figure 33. The beam and extractor currents

the user realized this would not be a good operating setting for this thruster.

After this amperage steadied for over 5 minutes the thruster was set to the operating voltage: beam 9 kV and extractor -1 kV. At this setting the beam and extractor currents returned to the baseline levels.

With the thruster passing the short circuit test, the thruster operated under closed loop beam current control with the setting of 20 µA. This gave the valve the necessary voltage increase to open and permit the flow of fuel. The thruster electronics increased the voltage to the microswitch in slow increments to prevent flooding the emitter surfaces due to the non-linear propellant flow response. Figure 34 and Figure 35 show the recorded microvalve voltage (blue) as well as the current to the beam (green) and extractor (red) required to maintain the operating voltages. After the 45 minute mark the fuel reached the surface and flooded the grids, causing a short. The thruster's electronics started to remove the voltage to the switch but eventually shut down to prevent any serious hardware issues.

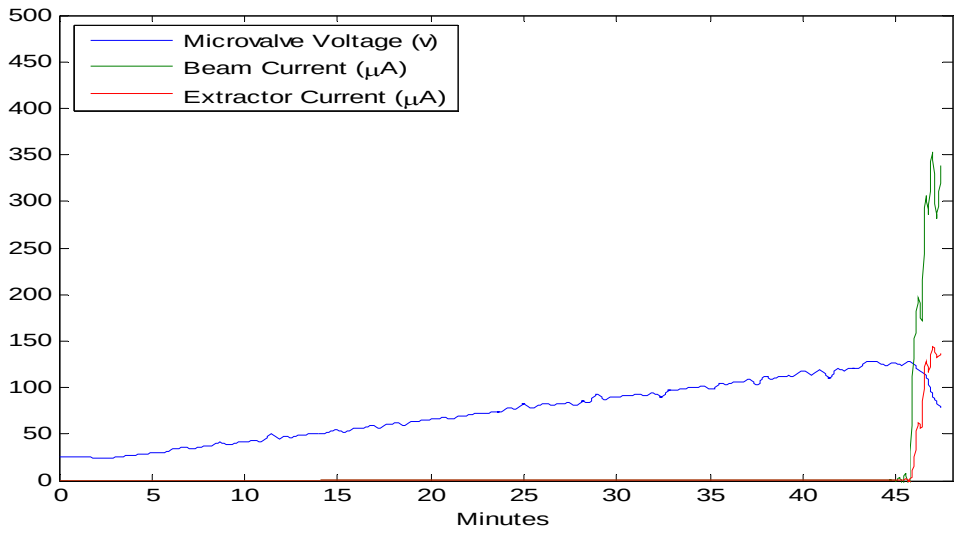

Figure 34. Key telemetry as the fuel flow started in priming the thruster

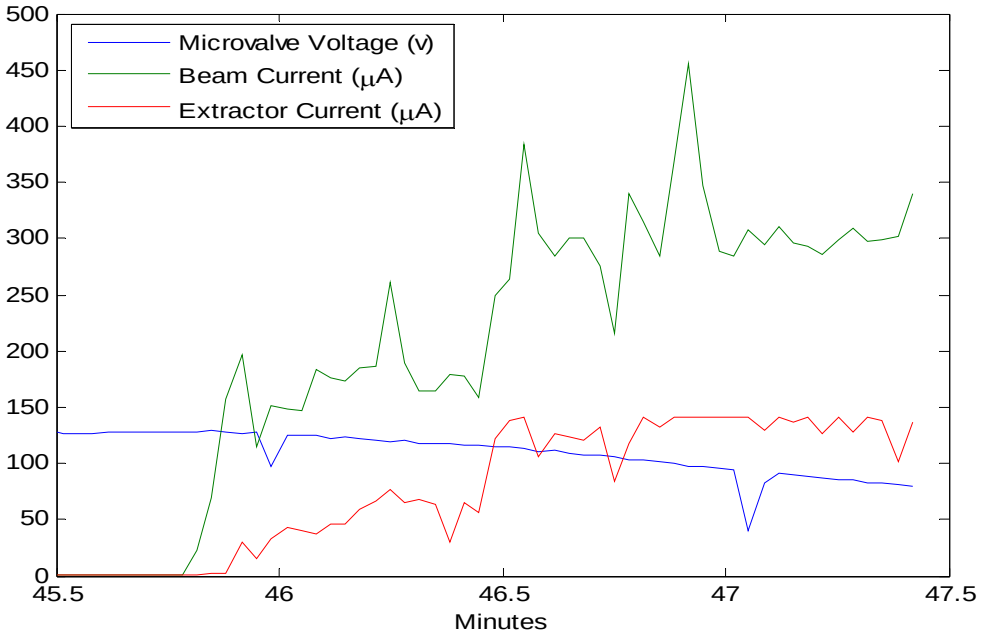

Figure 35. Close up of telemetry when the fuel finally reached surface of emitter

The thruster sat in the vacuum for an hour to allow the excess fluid to boil off before the commanded restart. Now this thruster was installed properly in the AFIT GNAT laboratory. The beam and extractor voltages were set at the operating levels and the propellant was primed for use.

4.2 Ensuring Proper Thruster Operation

The author had operated the thruster now at both the Busek Company and AFIT. By analyzing the data from both locations, a reasonable correlation meant that the thruster was operating properly at AFIT. The key recorded telemetry to aid in this analysis was the beam current, the extractor current, and their response to the valve movements. The flow of current of the beam and extractor corresponded to the charging and accelerating of the ionic droplets for thrust.

While ensuring the operation of the thruster before delivery, the author and personnel at the Busek Company ran the thruster in a closed loop beam current control logic where the CPU for the thruster regulated the fuel microvalve to try and maintain a steady 20 µA in beam current. The voltage of the fuel microvalve controlled by the CPU within the electronics package ramped up the mass flow rate of the fuel incrementally by adjusting microvalve voltage up slowly. If the CPU detected a short or other anomalies, the microvalve would be closed automatically.

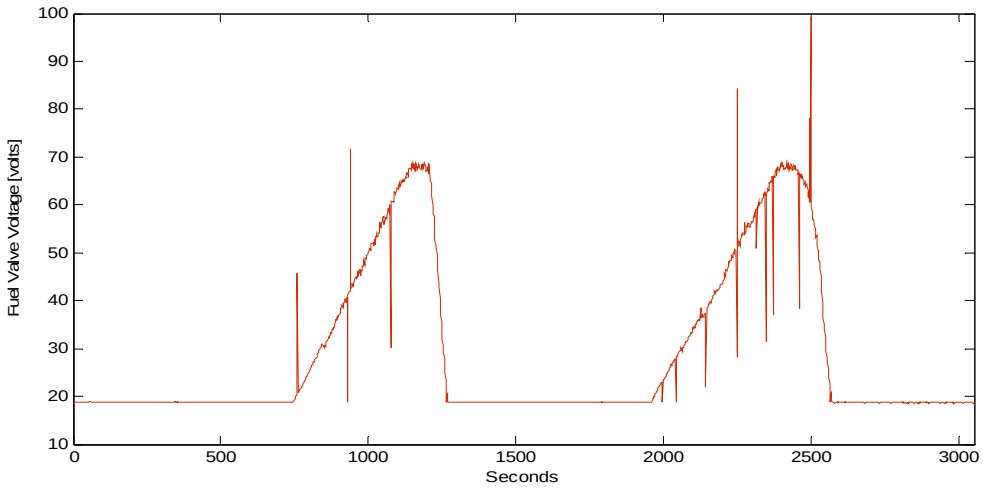

Figure 36. Voltage supplied to the microvalve to regulate fuel flow

Figure 36 shows two startup cycles in fuel mass flow rate (red). The baseline of 18 volts was the microvalve in its shutoff condition, where the microvalve is closed. From this base the electronics of the thruster applied increasing voltage to the microvalve to increase the mass flow rate of the propellant to the emitter surface. As more ionic liquid was drawn from the emitter surface, the PPU adjusted the current to maintain the beam voltage at 9 kV. When the beam current reached its target goal, the voltage to the fuel microvalve steadied. When the electronics detected an electrical discharge into the

plume, the voltage supplied to the fuel microvalve went directly down to the corresponding closed position.

Each cycle terminated abruptly due to a discharge of electricity into the droplet or ionic plume. The discharge occurred because the vacuum pressure within the chamber rose to above $1x10^{-6}$ torr. Discharges like this are known to happen to other types of colloid thrusters as well at these pressures. With the voltage increased, the fuel valve responded accordingly, and the pressurized fluid started flowing through the valve.

The control of the valve's displacement was linear, but the flow through the valve was not. This non-linearity was caused by the hydrophobic properties of EMI Im and the resistance of pressurized flow through the porous membrane. Miniscule amounts of water vapor formed on the fuel line walls when exposed to the atmosphere during construction and storage. The combination of water vapor and fuel formed small bubbles. These bubbles affected the rate of change in mass flow to the emitter site due to bubble compression and then migrated toward the porous emitter face.

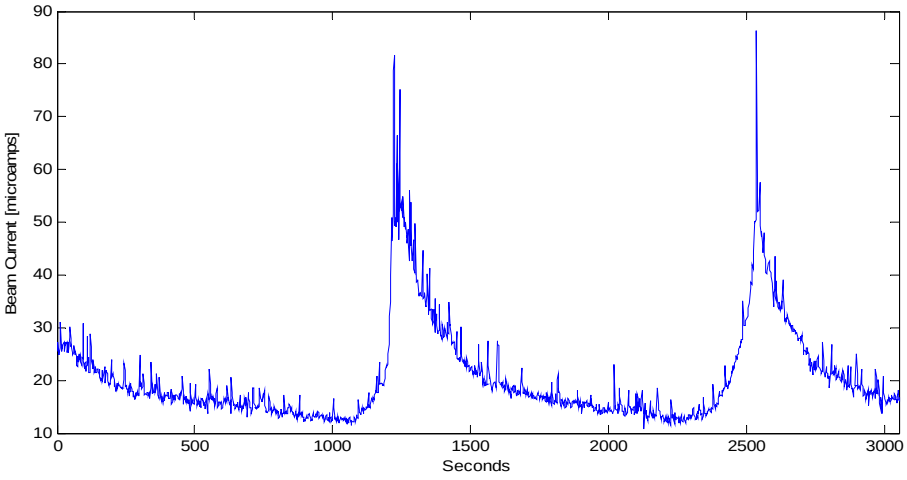

Figure 37. Beam current during the fuel valve operation

The beam and extractor current were good indicators of what was happening on the surface of the thruster. Figure 37 shows the beam current required to maintain the constant 9kV beam during these two startup cycles described in Figure 36. The peaks of over 80 µA represent the thruster discharging into the plume.

Figure 38 shows the current required to maintain the -1kv extractor during this same period of time. The overall shape of the plot is similar to the beam current found in Figure 37. The large spikes most likely represent bubble formation popping on the surface of the emitter. As the pressure in the lines decreased, the bubbles were pulled through the porous emitter by the capillary force. The other spikes are most likely caused by large fluctuations in the Taylor cone formations on the emitter surface.

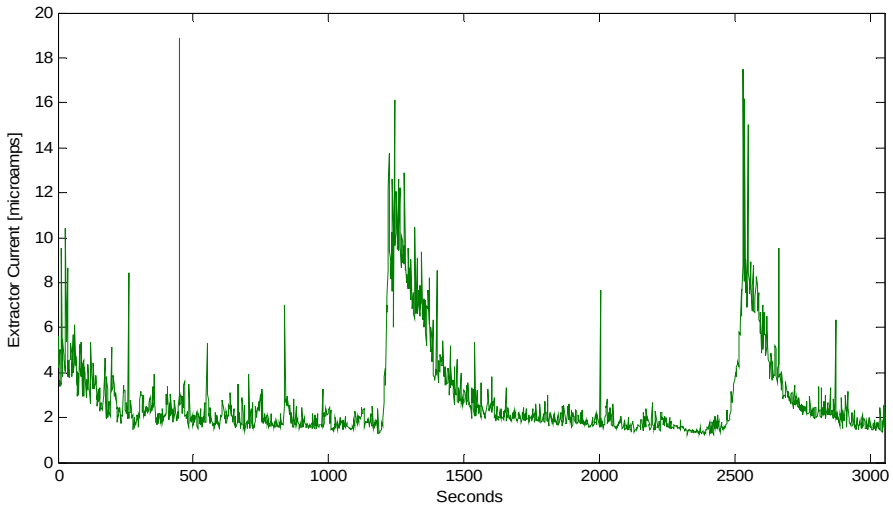

Figure 38. Extractor current during the variation of fuel flow rates

After the switch was closed, the vacuum chamber pumps started to lower the pressure within the vacuum again. The slow decay of amperage after these peaks represented the thruster expelling charged droplets of the ionic fluid. The flow of fuel through the porous surface had not stopped even though the microvalve to the fuel source

had been closed. The fuel continued to expel through the porous surface due to its capillary effects and residual pressure in the lines. As some of the bubbles worked through the holes to the surface, they popped, causing an abnormal emission to happen at that moment. This liquid was also charged by the beam current and was accelerated to the extractor as it was expelled from the thruster. The varying sizes of the droplets and the varying number of emissions sites at any given moment affected the current to the beam and extractor.

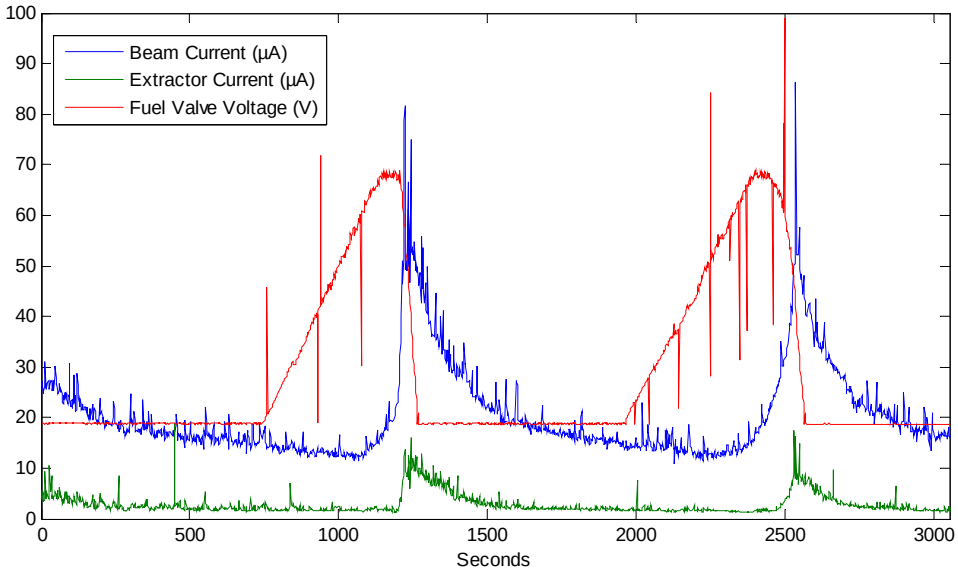

Figure 39. Beam current, extractor current and fuel valve voltage

Figure 39 and Figure 40 displays the three previous plots combined to better demonstrate the system response to the fuel microvalve voltage. There was a delayed system response between the adjusted voltage to the microvalve and the responding current fluctuations in the beam and the extractor. This delayed system response added difficulty in gaining proper control of thruster operation. As the thruster operated in the chamber over long periods of time (hundreds of hours), the bubbles worked their way out

of the fuel lines and through the emitter surface. According to the manufacturer, this thruster was operating normally within the vacuum chamber deficiency of maintaining vacuity.

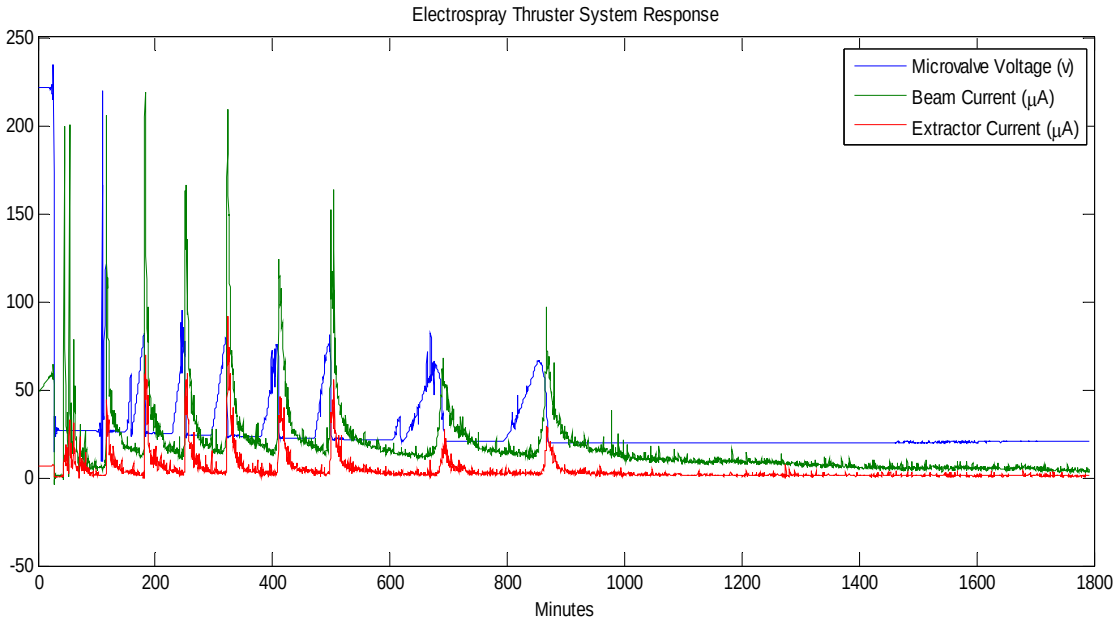

Figure 40. Key telemetry for the electrospray thruster operated at Busek

To ensure that the thruster was operating properly at both sites, the same experiment needed to be done at AFIT. As mentioned in Section 4.1, the thruster was primed and allowed to rest before this run. The thruster was again operated under closed loop beam current control with the setting of 20 μA until around the 500 minute mark where the fuel microvalve was commanded to the closed position of 17 volts.

Figure 41 displays the key telemetry of the thruster operation. The blue line represents the voltage (V) to the microvalve in regulation the flow of EMI Im to the emitter surface. The green line is the beam current (μA) needed to maintain the beam voltage of 9 kV. The red line represents the extractor also known as the accelerator current (μA). The currents continued to fluctuate well after the fuel valve was closed.

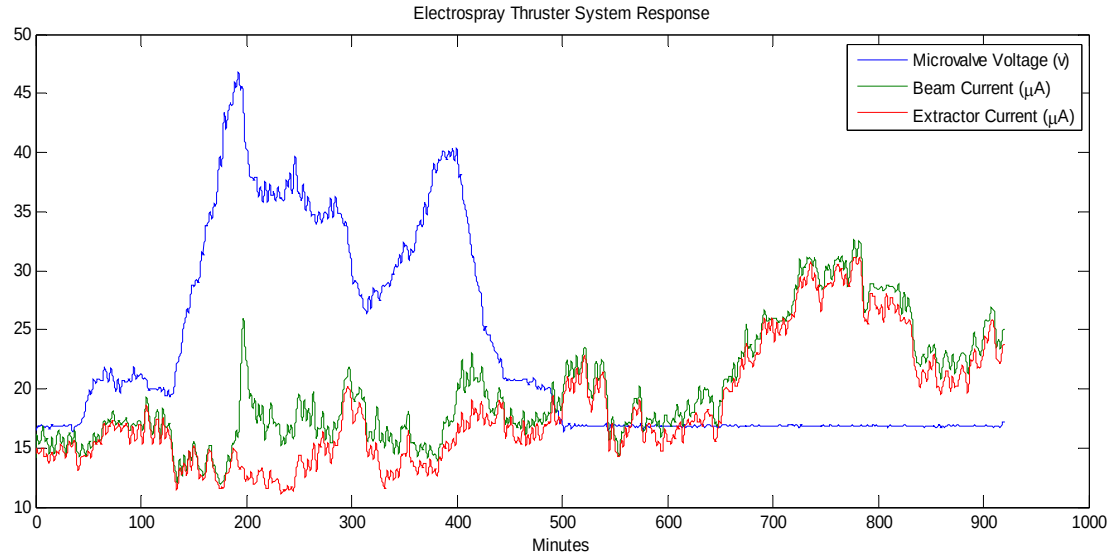

Figure 41. The key parameters of the electrospray thruster, beam current set at of 20 μA

Even though the fuel valve was closed, the flow through the emitter continued and the necessary current to maintain the beam and extractor voltages adjusted accordingly. With this beam and extractor current, the thruster was producing thrust. The actual produced thrust is unknown but the thruster electronics provided a rough order of magnitude of its produced thrust calculation.

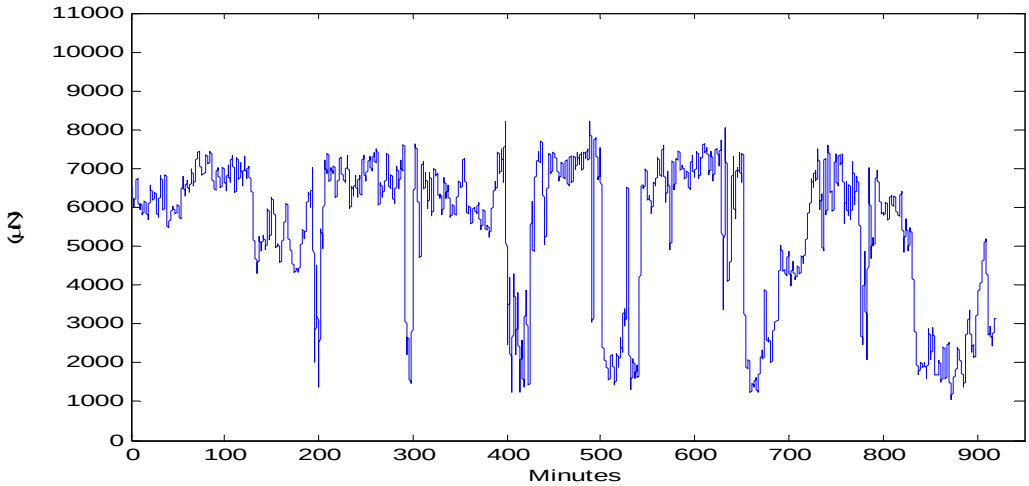

Figure 42. The calculated thrust by the CPU of the thruster

This calculated thrust seen in Figure 42, is not even in the ball park of the actual produced thrust of the thruster. This graph has no apparent relation to Figure 41, even with them covering the same experiment. The calculated thrust feature was created for future use. When installed on a satellite the commanded thrust level would be the primary method of operating the thruster instead of using the closed loop beam current command. This feature required calibration and was not used from this point in the experimentation, but the thrust was also calculated using the recorded telemetry.

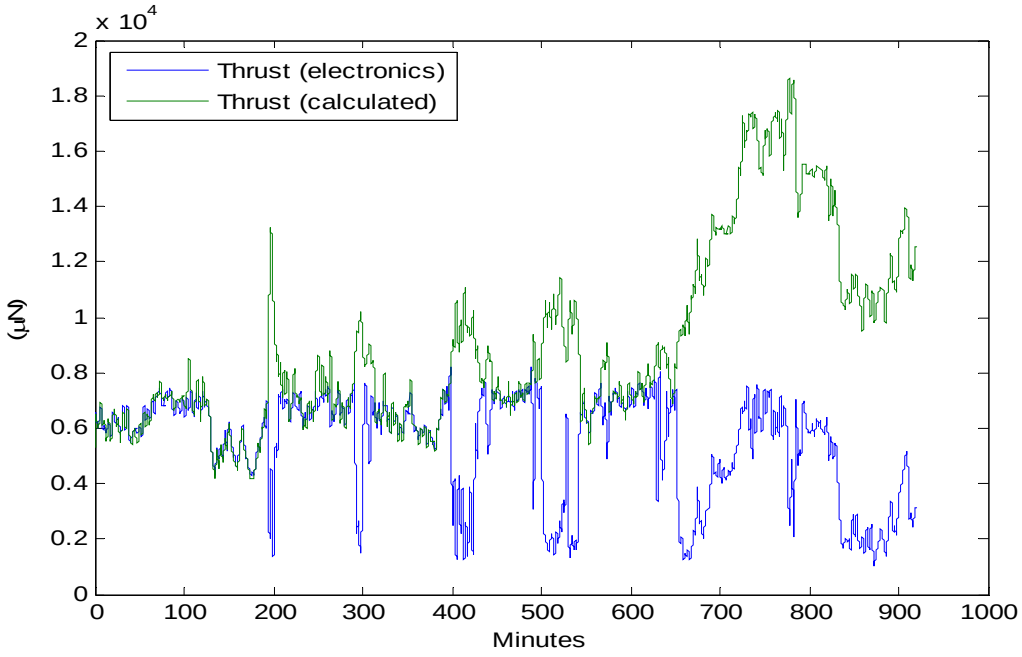

Figure 43. Calculated thrust from equation 2.7 (calculated) and by the electronics

With the beam current recorded, the thrust was calculated using equation 9 from section 2.7. V_a was set to 10 kV and the I_B was the recorded beam current. C_n was manipulated to get the graphs to line up and the final value used was 1. Figure 43 illustrates both calculated thrusts. Because thrust is dependent on the beam current, the green line follows the same trends as the beam current from Figure 41. This is a rough

calculation and may not correlate to the actual produced thrust, so this calculation is not used for the rest of this thesis.

With the commanded beam current set at 20 µA, the thruster electronics started incrementally increasing the propellant microvalve's voltage to initiate the flow of fuel. As seen in Figure 44, this operation started at the recorded 130-minute mark and the beam current's first real response started at around the 60 minutes later.

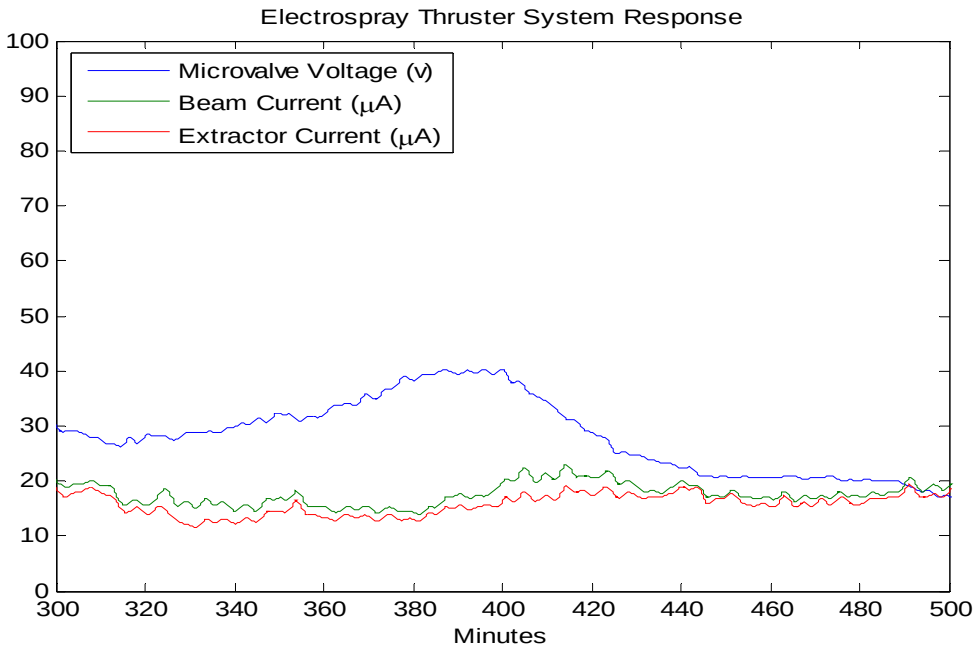

Figure 44. The key parameters of the thruster zoom-in from Figure 41

After the initial beam response the thruster settled into a smooth operation in maintaining the beam current around the desired 20 µA. Figure 45 displays a zoomed-in image showing the thruster adjusting the valve voltage to maintain this beam current. The spikes in the readings may be stray voltages being picked up by the sensitive sensors. Until this phenomenon is better understood, the author will not attempt to include it in the analysis.

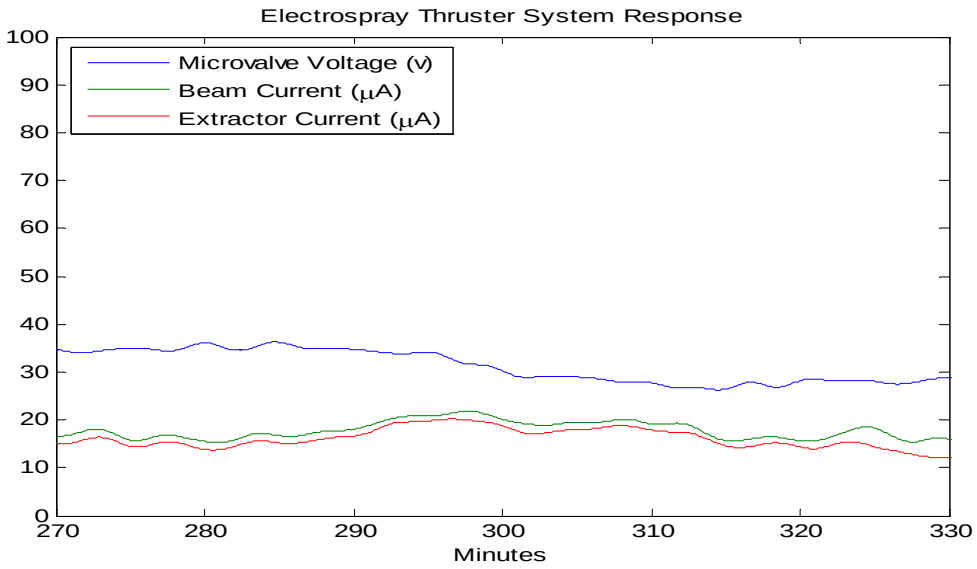

Figure 45. The key parameters of the thruster zoom-in from Figure 44

Note that the beam and extractor currents follow very similar responses. This goes back to the original understanding of how colloid thrusters work. The beam current was used to pull the ionic droplets/molecules from the emitter surface through the formations of Taylor cones. The extractor accelerated these ionics further into producing the thrust. The combined number, size, and level of charge of these droplets corresponded to the required current to maintain the voltage differences. Since the beam and extractor experience the same ionic droplets, they should have similar responses as well.

The thruster operation at AFIT went more smoothly than the same operation at the Busek Company. The use of the bell vacuum chamber was ideal in the operation of this colloid thruster. The initial vacuum pressure was 5.6×10^{-9} torr and rose to 6.5×10^{-7} torr when the thruster operated at the highest flow rate. With the pressure so low, the

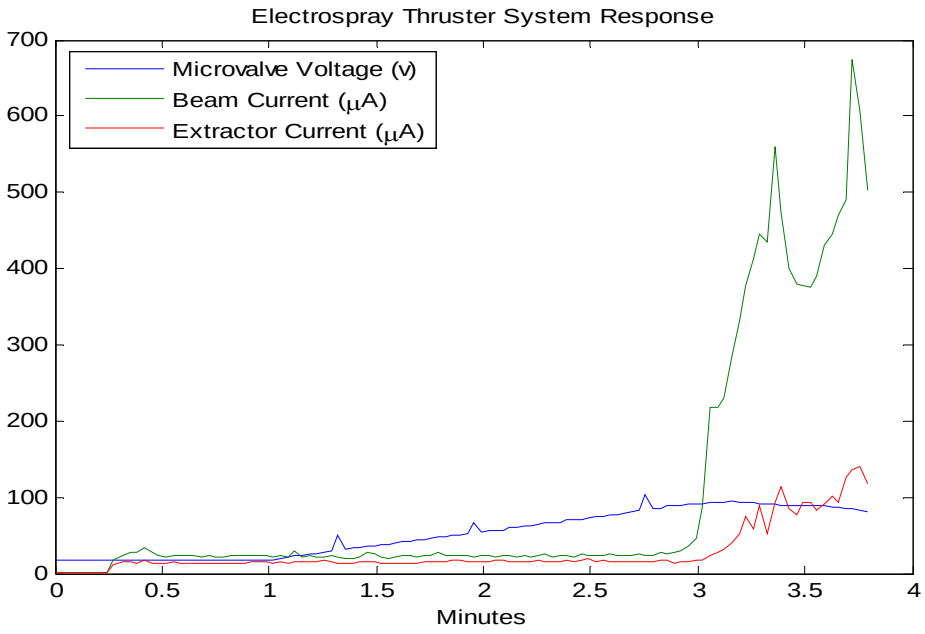

Figure 46. The telemetry of second run with beam current set to 300 μA

thruster never discharged the voltage field into the droplet plume. For this major reason, the thruster never got into the cyclic operation observed at the manufacturer's facility.

Once this one-of-a-kind electrospray thruster worked at AFIT, the thruster was set to a higher beam current of 300 μA, to check the range of the pumping capability of the chamber. This run lasted only 7 minutes until the com-channel dropped between the thruster electronics and the LabVIEW interface. Figure 45 show the key telemetry of the thruster, the microvalve voltage (blue line), the beam current (green line) and the accelerator current (red line). The flow through the emitter increased the current until the beam spiked, at which time the voltage to the microvalve decreased.

With the power to the com-channel restored, the user brought the thruster back to the correct beam and extractor voltages. The run was tried again with the closed loop beam current set to 300 μA, and Figure 46 shows what happened. The telemetry is the same as before with the microvalve voltage (blue line), the beam current (green line) and the accelerator current (red line) being shown. This time the run lasted under four

minutes. The impingement warning light lit up in LabVIEW, meaning an unsafe amount of current was required to maintain the beam voltage. This was possibly due to the instillation angle of the thruster at AFIT. The chamber vacuity never fell below $6.5x10^{-7}$ torr during these runs.

With these impingements, the author decided to operate the thruster at a lower targeted beam current. Figure 47 shows the results when the thruster current was set to 150 µA, then changed at the four-minute mark to 100 µA because the impingement warning light flared again. Then the com-channel failed again.

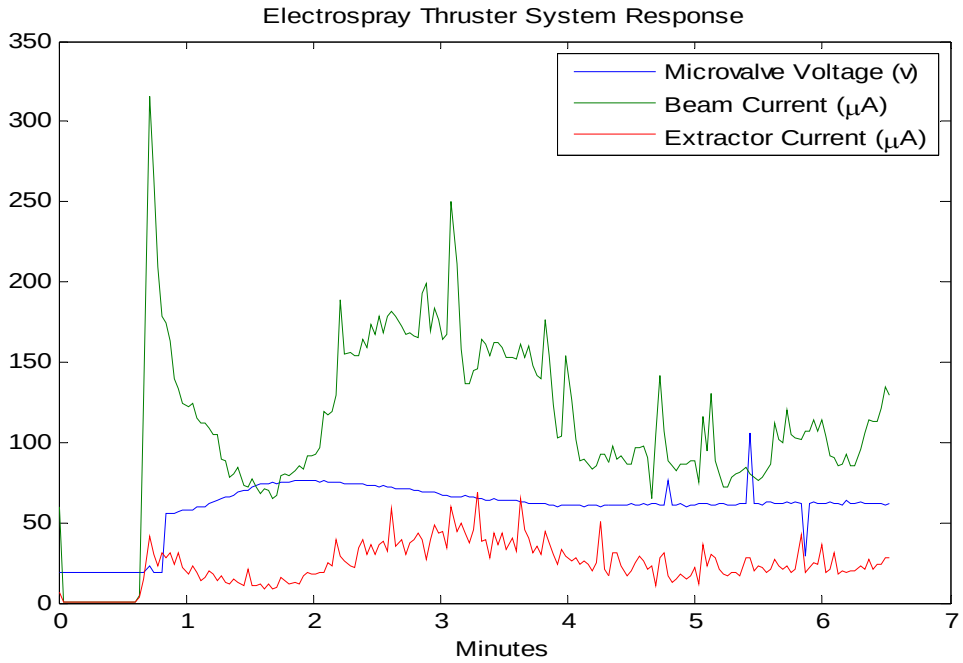

Figure 47. Telemetry of beam current set to 150 µA than 100 µA

The thruster continued to operate and the com-channel was restored. Figure 48 shows how the system appeared to recover at the 1.5 minute mark. So the thruster was given 40 µA as the target for the beam current. The com-channel again failed.

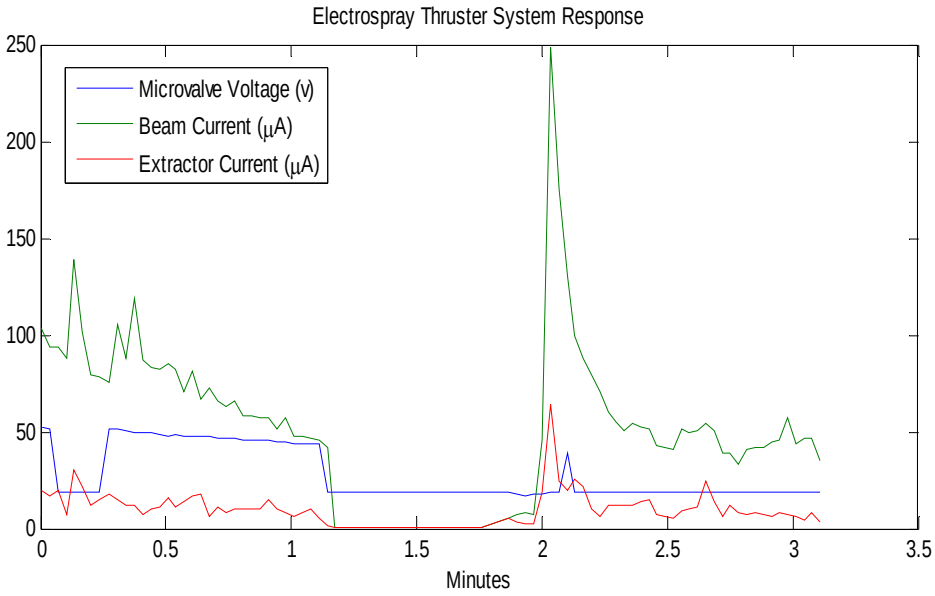

Figure 48. The telemetry after com-channel was restored

The com-channel was restored again and after a while the beam current was set to 40 μA again.

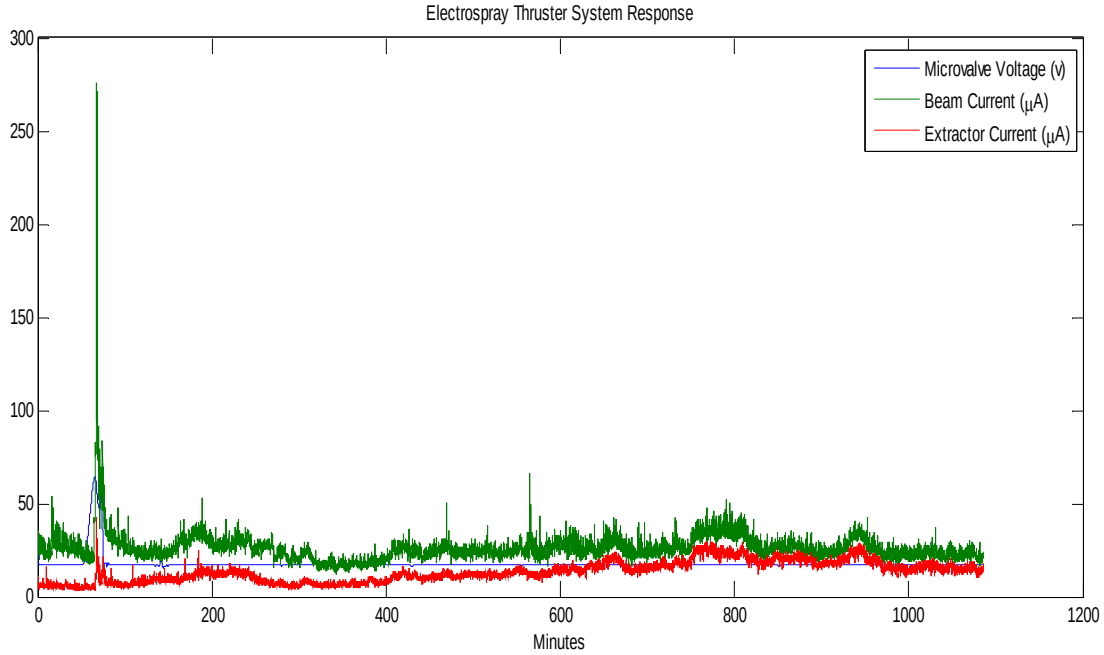

Figure 49. Thruster operation while clearing the impingements

Figure 49 shows the thruster operation on this run. When the impingement warning light returned, the user commanded the thruster to close the fuel's microvalve (see Figure 50). The thruster then sat in the chamber for over 16 hours so the surface had time to allow the fuel flow to the emitter surface to stop. The excess pressure within the fuel lines and the capillary effects due to the porous emitter caused the fuel to continue to flow. According to the operating manual, the beam and extractor currents should be minimal.

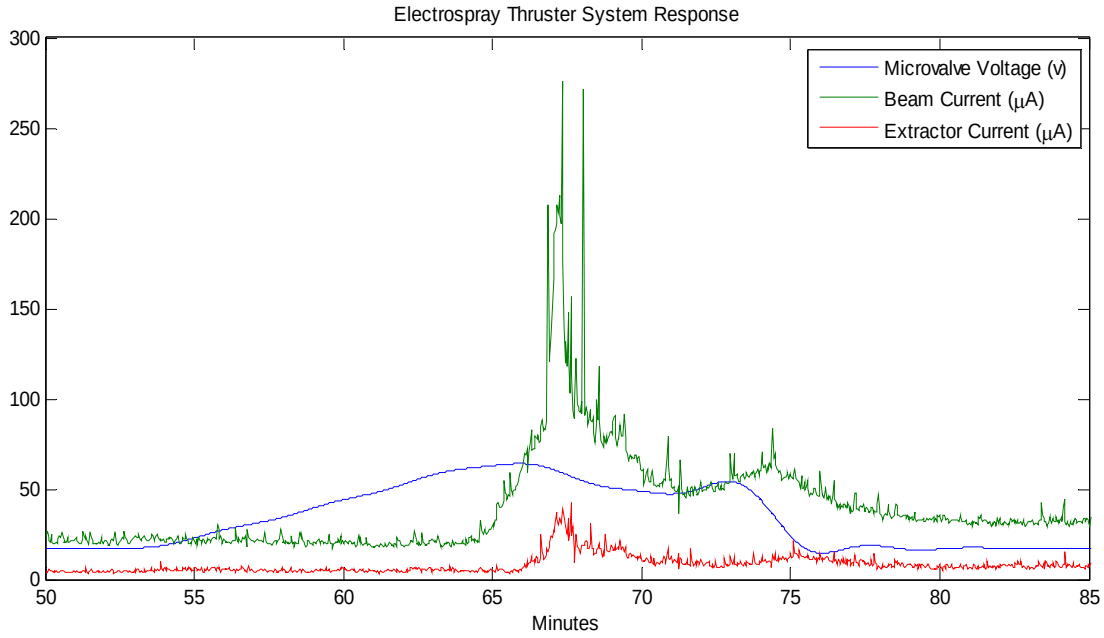

Figure 50. The thruster telemetry of the commanded beam current of 40 μA

After all of these runs, continued proper functioning required the emitter surface to be cleaned. Figure 51 illustrates that when the chamber was opened, a black discoloration covered two of the nine emitter surfaces. This discoloration resulted from the thruster impingements, the flooded fuel shorting out the beam to the grounded field.

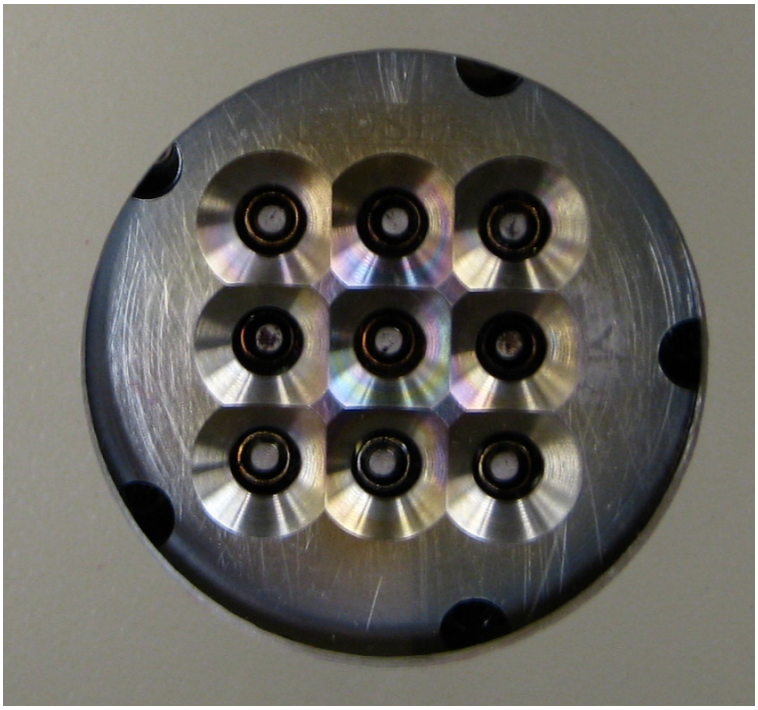

Figure 51. The thruster after operation. Note the discoloration on some of the emitter surfaces

4.3 Capturing Taylor Cone Formations with Varying Flow Rates

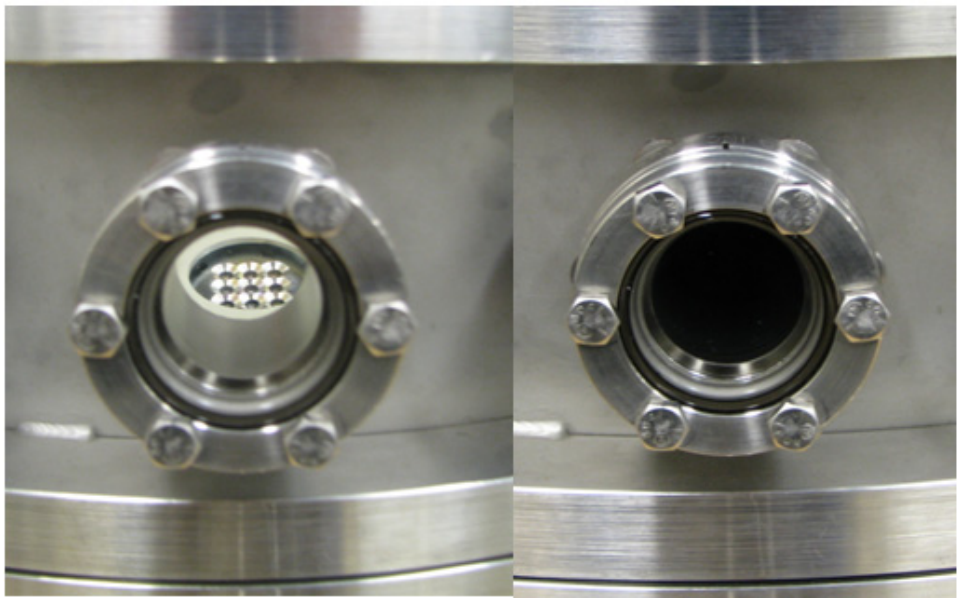

Figure 52. The vacuum chamber window used for Questar camera system

Figure 52 shows the vacuum chamber window. The image on the left shows the image with the chamber opened, allowing the light within the laboratory to illuminate the thruster within the vacuum chamber. The image on the right is of the window with the vacuum chamber closed. There are two panes of glass for this window.

The focusing of the Questar's QRMS-II camera system through the windows of the chamber failed. The use of different telescope components and a converging lens did not overcome the problem. Figure 53 illustrates the overall situation with the laboratory set up with the camera system.

Figure 53. The Questar QRMS-II camera system

The author focused the Questar QRMS-II camera system on the center emitter surface before the chamber was closed for the thruster operation. Once the operation of the thruster was under way, the camera system was turned on to capture images of the emitter surface. As described in section 3.6.3, the camera computer interface can control

the fine movement of the system to make the final focus. A search pattern was used by setting the x (side motion) and then the y direction (up down motion). The z was allowed to move in and out. This was repeated while the author observed the image on the computer screen.

After several attempts, the camera system could not focus on objects inside the chamber. With the reported runs completed, the chamber was brought back to atmospheric condition. This time with the chamber bell lifted off the base, the author attempted to get an image of the emitter. Several tries failed to achieve adequate focus. The author then targeted the camera on a bolt on the outside of the chamber window, using the prescribed method. The camera was focused on the bolt with this method in under one minute. Yet all attempts in getting an image though the window failed.

In summary the one-of-a-kind electrospray thruster operated successfully at both the Busek Company and AFIT. While operating at the Busek facility the vacuum had difficulty in maintaining vacuity, causing the electric fields of the thruster to discharge into the ionized droplet plume. When operating within the AFIT facility the thruster operated stably at the low beam current setting. However, at the higher corresponding flow rates the thruster impinged. This impingement likely is related with the thruster being installed into the chamber at a twenty degree slope. The Questar QRMS-II camera system failed to take images of the Taylor cone formation on the emitter surface.

V. Conclusions and Recommendations

This chapter presents the preliminary conclusions found through the research and experimentation on the electrospray colloid thruster. It discusses possible solutions to identified problems and methods to avoid further potential problems. It also puts forward a possible hardware change for future models of this type of thruster. As this experiment demonstrates, with the electrospray thruster using a unique system in forming the Taylor cones in operation, there is a broad range of possibilities for further study.

The operation of the thruster was successful and is a big step in getting this type of electric thruster onto an AFIT CubeSat. The operation of the electrospray thruster met two of these thesis objectives: operate the electrospray thruster at AFIT and ensure that the thruster is operating properly. The thruster operated properly at the low fuel flow rate with the thruster beam current settings set to 20 µA. At this flow rate, the AFIT bell chamber allowed far smoother system response of the thruster operation compared to the thruster operation at the Busek Company.

The major factor in the smooth system response is due to the vacuity of the chamber. Where the Busek Company's chamber pressure went above 1E-6 torr, the AFIT bell chamber never exceeded 6.5×10^{-7} torr. When a colloid is operated at pressure above 1×10^{-6} torr, the electrical fields short out into the droplet plume.

While operating the electrospray thruster at the Busek Company, there was a fine balance between mass flow rate and the maintenance of the chamber vacuum to prevent an electrical discharge in the fuel exhaust plume. With the vacuum pump having a difficult time maintaining vacuity, the thruster could only operate at very low fuel flow

rates. Once stabilized, the fuel microvalve setting could be set, leading to the flow of the fuel and the start of the next run.

The operation of the thruster at AFIT worked well at this low fuel flow rate with no electrical discharges into the plume. But the thruster experienced several impingement events while operating at higher flow rates. The thruster electronics were programmed to shut down under these conditions to protect the thruster's hardware from serious damage. This shorting of the beam voltage to the floating ground of the thruster arose because the ionic fluid came in contact with both of these surfaces at the same time on at least one of the nine emitters.

The major culprit of the impingement seen during operation was due to the flooded thruster while the thruster orientation was at twenty degrees off vertical. In the illustration in Figure 54, the dark blue represents the propellant. The left image shows the formation of ionized droplets in low flow conditions. As the flow increases, the formation of propellant grows and eventually the fuel shorts out the beam to the grounded ring that surrounds the porous emitter. The black objects represent the extractor charged to -1 kV.

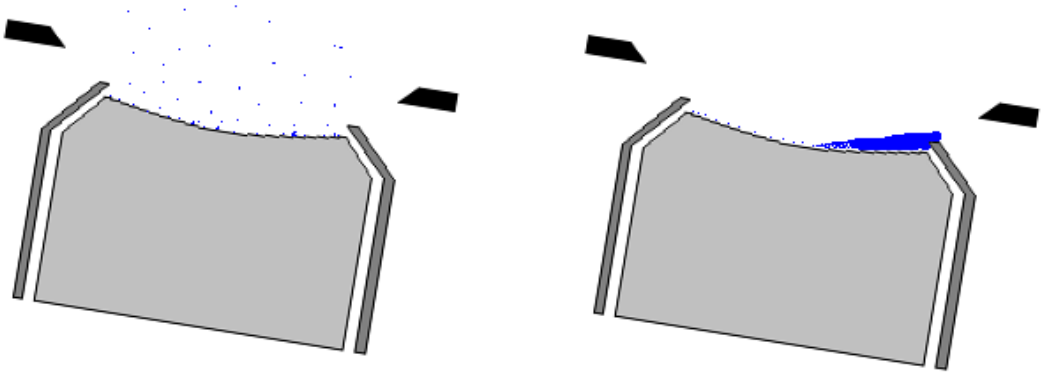

Figure 54. Illustration of the porous emitter surface while in operation

As the thruster operated in the low closed loop beam current setting, the Taylor cones formed within the voids of the upper porous surface. As the fuel rate increased, more and more of the propellant coated the emitter surface. Eventually the excess fluids pooled together and flooded onto the neighboring grounded surface. When this occurred the warning impingement light illuminated, and eventually the thruster electronics shut down the operation to protect the hardware from serious damage.

Figure 55 shows how the pool of fluid forms with the thruster in the proper vertical orientation. With this orientation, the pool allows for the formation of Taylor cones on the upper surface of the propellant. Even in this orientation, the thruster could experience the impingement, but far greater liquid needs to form on the parabolic emitter surface.

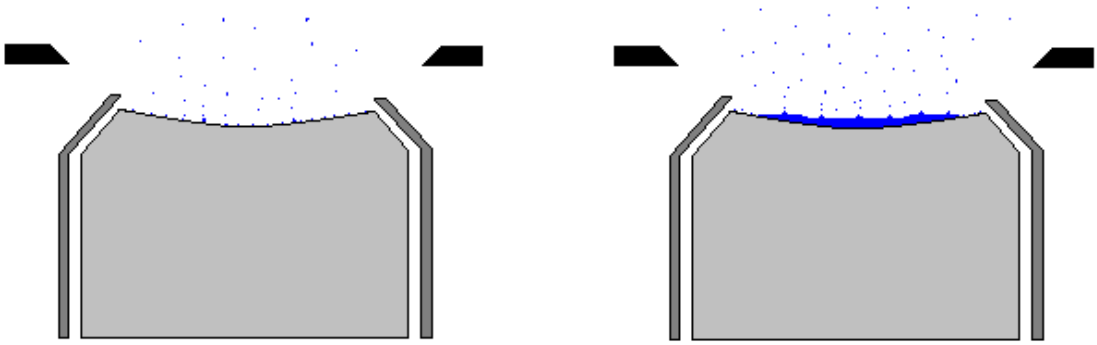

Figure 55. The emitter functioning in the proper vertical orientation

As with installing the thruster in the proper orientation, there are several other recommendations for operating the thruster and for future work to be done. The next few paragraphs cover these recommended improvements to the thruster. The possible upgrades to the vacuum chamber are also discussed.

Another area that needs to improve is the onboard-calculated thrust. This thrust value is only a guide at this point. When the thruster is properly calibrated to true thrust,

it may be more advantageous to use. There are some issues that probably need to be addressed to make this thrust calculation more reliable. During the experiments the pressurized fuel tank was filled with filter nitrogen. The use of this inert gas may be used for short term testing, as the change in volume around the outside of the bellows will not change significantly, resulting in minimal loss of drive pressure. For operations lasting longer than 100 hours, the tank should be permanently connected to an external pressure source or filled with a vapor pressure liquid, such as butane, to maintain pressure.

To make the thrust calculation far more reliable, a pressure gauge should be used to measure the pressure of the tank at the time of calculating the thrust. The movement of the piezo-actuated microvalve is relatively linear but the actual fuel flow is nonlinear. This flow rate is a function of the pressure found within the fuel tank, the amount the valve is open, the resistance and the capillary effect of flow through the porous emitter. Then a proper correlation could be made with the calculations having this data with calibrations to actual thrust measurements. Without the fuel tank pressure, this calibration would be a moving target. This thruster should get a pressure gauge built into the fuel tank subsystem.

The next issue that needs to be addressed is the vacuum chamber at AFIT. As mentioned earlier the camera system never did focus on any object within the chamber. The QRMS-II uses a pulsed light source that travels down the same pathway as the image returns. This is not an issue when traveling through air, but when light travels through the two planes of glass of the chamber window and back, the primary desired image is lost. The major reasons for the loss of function is, first, the glass has no antiglare coatings; and second, the camera system is set at a non perpendicular orientation to the

glass panes, and pulsed light timing may interfere causing the refraction of light to hit the opposing surface of the glass panes. This refraction interfered with the exposed light of the target when its return image hit the camera sensor.

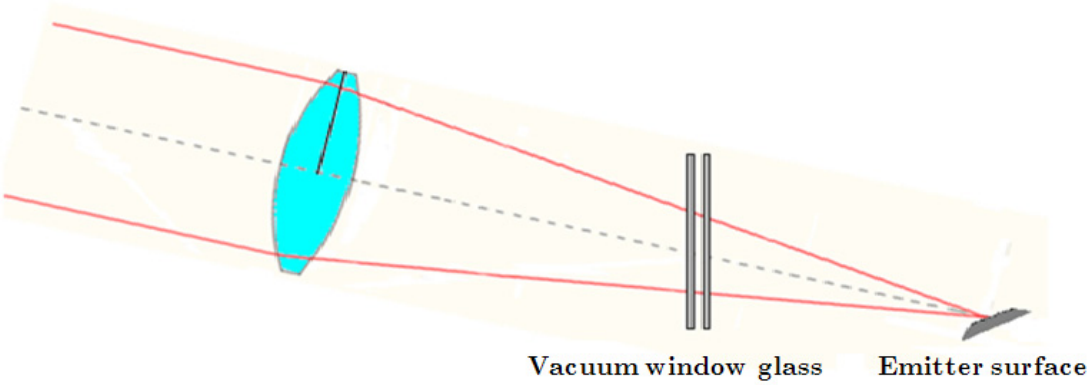

Figure 56. Illustration of optics path though chamber window

With this knowledge, the Questar QRMS-II camera system might work if a light source can be placed within the chamber itself. This would overcome the refraction of light on the same path as the desired image. It is also recommend to have an antireflective coating on the window panes. With these changes, the Questar QRMS-II camera system should be able to capture the images of Taylor cone formations.

After possible upgrades to the hardware, the next step is to consider the future work which needs to be done with this research. The experiments of this thesis have demonstrated a sensitivity in the thruster operation necessitating a proper orientation because of the influence of gravitational forces. The easiest way to overcome this issue in future experiments is to operate the thruster facing directly up and directly down while capturing the thrust in the vertical directions. Another recommendation is to closely monitor the different corresponding stable fuel microvalve voltages while operating in

these two different orientations. This will only aid in understanding some of the gravitational effects on the thruster's operation.

Further study will need to perform finite element analysis of the forces on the surface of pooled liquids in a micro gravity state of space. A question to answer is how will the fuel's pooling in this space environment on the emitter surface correspondingly affect the operation of the thruster? How much will this variance affect the produced thrust of the thruster, and can the thruster electronics be better calibrated to reflect the actual microgravity performance.

Another area of research is the operating envelope of the electrospray thruster by varying beam voltage. For the current experiment, the operation of the colloid thruster was limited to the manufacturer's recommended setting of beam voltage at 9 kV. With the thruster operating at different flow rates, a more conducive beam voltage might be found. An optimal operation of fuel flow rate and beam voltage then could be mapped to optimize the operation of this thruster.

From this work, the thruster operation algorithms could be optimized within the thruster's electronics package. This would then be a stable operational thruster. From this point, it would be ideal to capture the key performance characteristics: thrust, specific impulse, and the thruster's overall efficiency. Other items that would aid in understanding this thruster are measuring the droplet flow divergence from the thruster and the size and velocity of the EMI Im droplets.

The current thrust balance found at AFIT could only work with the thruster operating at very low fuel flows and oriented off vertical. Since this would not work at higher fuel flow rates, and to capture more accurate readings of thrust, a vertical thrust

balance should be developed. This thrust stand could be built using the same type of hardware found on the current torsional balance but be optimized for vertical orientation.

One feature that would need to be added to this balance is the adjustment of the capacitor distance while the chamber is under vacuum. The calibration of the balance stand requires these capacitors to be at a certain distance, yet the distance sometime drifts while the chamber is brought down to vacuum. Where the ability to drift would increase with the vertical orientation, this would be critical due to the probability that this drift would cause the capacitors to touch and would need to be corrected after the chamber is already in the low-pressured state.

This concludes the recommended future work with the thruster and leads to the key recommendations. The key recommendations in the operation of the thruster are as follows:

- Operate the thruster in a vacuum chamber that can maintain vacuity of at least $1x10^{-6}$ torr at all times. This will ensure that the electric fields will not discharge into the droplet plume.
- Operate the thruster in the vertical orientation only. This orientation will limit the impingement of the thruster to highest flow rates.
- Ensure all wiring can withstand the high voltages and solder the lines together. Do not use alligator clips or BNC connectors.
- Place c-clamps on the bell chamber. This step allows the bell vacuum chamber to achieve lower vacuum pressures.
- When the impingement light goes off several times in a short period, clean the thruster using the manufacturer's directions before operating the

thruster again. The buildup of solidified charred EMI Im on the surface may be causing the impingement and will come off using the cleaning agent.

- Do not rush in the initial voltage hardware test. This may lead to unnecessary short circuits in the wiring or harm the hardware permanently.

In summary, the electrospray thruster is the first electric thruster seriously packaged to go on a 3U CubeSat. This work has shown that the thruster and the included electronics work as advertised. The thruster's unique approach in the formation of Taylor cones worked and allowed for far greater range of thrust capability. With the porous emitter, there are complex interaction of forces in the formation of ionized droplets.

The operation of this unique thruster also demonstrated the ease of use and the reliability and built-in safety of the thruster electronics package. The use of the Flourinert electronic liquid kept the PPU and DCIU from shorting or overheating. Before this current packaging, the power converters covered several racks.

The foundation work performed for this thesis should aid in the further refining of the operation of this electrospray thruster. The use of the GNAT bell vacuum chamber allowed enough vacuity for the full operation of this thruster. The thruster has operated properly at Busek Company and at AFIT. The ability to study and capture the performance parameters of this thruster may one day allow this type of thruster to be used on a future AFIT 3U CubeSat and meet some of the USAF space capabilities shortfalls.

VI. Bibliography

[1] ----. *1U Colloid Thruster & Electronics Operation Manual.* Natick, MA : Busek Co Inc., 10 November 2010.

[2] Connolly, Young, Hruby, Demmons, McCormick, Gasdaska, Spence and Rhodes. "Power Processing and Control DRS Colloid Thrusters," AIAA 2004-3597, 2004.

[3] Debevec, J. *Vacuum Chamber Construction and Contamination Study of a Micro Pulsed Plasma Thruster*. MS Thesis AFIT/GAE/ENY/07-D01. Air Force Institute of Technology (AU), Wright-Patterson AFB OH, Dec 2006.

[4] Demmons, Hruby, Roy, Martin and Spence. "Electrospray Thruster Development", AIAA Conference paper, 2009.

[5] Fenn, Mann, Meng, Wong and Whitehouse. "Electrospray ionization for mass spectrometry of large biomolecules," Science 246, 4926, 1989.

[6] Hruby, Gamero-Castano, Falkos, and Shenoy. "Micro Newton Colloid Thruster System Development," IEPC-01-281, 2001.

[7] Humble, Ronald W., Gary N. Henry, Wiley J. Larson. *Space Propulsion Analysis and Design*, New York, New York: McGraw-Hill Companies Inc, 1995.

[8] Jahn, R. *Physics of Electrical Propulsion.* Mineola, NY: Dover Publications, Inc., 2000.

[9] Krpoun, R. *Micromachined Electrospray Thrusters for Spacecraft Propulsion.* MS Thesis, Ecole Polytechnique Federale de Lausanne, Suisse, 2009.

[10] Martinez-Sanchez, M. "Lecture 23-25: Colloidal Engines", *URL:* http://ocw.mit.edu/courses/aeronautics-and-astronautics/16-522-space-propulsion-spring-2004/lecture-notes/November [cited 5 January 2010].

[11] Mills, A. and Chang, B. "Error Analysis of Experiments, a Manual for Engineering Students" 46-147 Engineering IV, University of California, 2004.

[12] Nabity, Mason, Engel, Daily, Lagumbay, Kassoy, "Studies of MEMS Colloid Thrusters," AIAA 2006-5007, 2006.

[13] Pranajaya, C. "Progress on Colloid Micro-Thruster Research and Flight Testing.", URL:

http://ssdl.stanford.edu/ssdl/images/stories/papers/1999/ssdl9912.pdf [cited 10 March 2010].

[14] ----. *Questar RMSII v4 Install and Setup.* New Hope, PA : Questar Corp., 17 July 2000.

[15] Randolph, T. and Ziemer, J. "Microthruster Propulsion for the Space Technology 7 (ST7) Technology Demonstration Mission," AIAA 2006-4320, 2006.

[16] Selstrom, J. *Thrust and Performance Study of Micro Pulsed Plasma Thruster*. MS Thesis, AFIT/GAE/ENY/10-M21. Air Force Institute of Technology (AU), Wright-Patterson AFB OH, Dec 2006.

[17] Stark, Stevens, Kent, Sandford, and Alexander. *Micro-Fabrication and Operation Nano Emitters Suitable for a Colloid Thruster* , URL: https://escies.org/GetFile?rsrcid=1094 [cited 10 March 2010].

[18] Urdiales, J. *Progress in Colloid Propulsion.* MS Thesis, Department of Aeronautic and Astronautics, Massachusetts Institute of Technology (MIT), Cambridge MA, September 2004.

[19] Zeleny, J. "Instability of electrified liquid surfaces." *Physical Review*, No. 10, 1917, pp. 1-6.

[20] Zeleny, J. "The electrical discharge from liquid points, and a hydrostatic method of measuring the electric intensity at their surfaces." *Physical Review*, No. 3, 1914, pp. 69-91.

Vita

Captain Scott T. Ober graduated from Barnum High School in Barnum, Minnesota. He served a two-year mission to Oakland-San Francisco California Mission for the Church of Jesus Christ of Latter Day Saints. He entered undergraduate studies at the Brigham Young University in Provo, Utah, where he graduated with a Bachelor of Science degree in Mechanical Engineering in April 2002. He was commissioned through the Officer Training School in April 2004 at Montgomery, Alabama.

His first assignment was at Tinker AFB as a sustainment structures engineer for the B-2 system program office. While stationed at Tinker, he deployed overseas in June 2004 to spend three months at Andersen AFB, Guam, as the B-2 on-sight engineer. In June 2005, he was assigned to the National Air and Space Intelligence Center, Wright-Patterson AFB, Ohio, where he served as an intelligence officer, flight chief and director of operations. In August 2008, he entered the Graduate School of Engineering and Management, Air Force Institute of Technology. Upon graduation, he will be assigned to the Air Force Research Laboratory at Edwards AFB, California.

REPORT DOCUMENTATION PAGE

Form Approved
OMB No. 074-0188

1. REPORT DATE *(DD-MM-YYYY)*	2. REPORT TYPE	3. DATES COVERED *(From – To)*
24-03-2011	Master's Thesis	Aug 2009 – March 2011

4. TITLE AND SUBTITLE

CubeSat Packaged Electrospray Thruster Evaluation for Enhanced Operationally Responsive Space Capabilities

5a. CONTRACT NUMBER

5b. GRANT NUMBER

5c. PROGRAM ELEMENT NUMBER

6. AUTHOR(S)

Ober, Scott T., Capt, USAF

5d. PROJECT NUMBER
11Y133

5e. TASK NUMBER

5f. WORK UNIT NUMBER

7. PERFORMING ORGANIZATION NAMES(S) AND ADDRESS(S)
Air Force Institute of Technology
Graduate School of Engineering and Management (AFIT/EN)
2950 Hobson Way, Building 640
WPAFB OH 45433-8865

8. PERFORMING ORGANIZATION REPORT NUMBER
AFIT/GAE/ENY/11-M22

9. SPONSORING/MONITORING AGENCY NAME(S) AND ADDRESS(ES)
Air Force Research Laboratories, Propulsion Directorate
Attn: Dr. Michael T. Huggins
5 Pollux Drive, Bldg 3353
Edwards AFB, CA 93524
(661) 275-5230 (DSN: 525-5230)

10. SPONSOR/MONITOR'S ACRONYM(S)
AFRL/RZS

11. SPONSOR/MONITOR'S REPORT NUMBER(S)

12. DISTRIBUTION/AVAILABILITY STATEMENT

APPROVED FOR PUBLIC RELEASE; DISTRIBUTION UNLIMITED.

13. SUPPLEMENTARY NOTES

14. ABSTRACT

A new specialized electrospray thruster with a potential to be used with a 3-U CubeSat was operated. The key difference in this thruster from traditional colloid thrusters is the porous stainless steel surface used for the emission sites. With this porous surface the actual location and number of the Taylor cones formations vary with changing fuel flow. The understanding of these formations is discussed with low, moderate, and high flow rates. The limitations of the experiment and observed system response are discussed. Due to these limitations, the colloid thruster was only able to operate in the low mass flow rate regime.

15. SUBJECT TERMS

colloid thruster, electrospray, Taylor cones, electric thruster

16. SECURITY CLASSIFICATION OF:			17. LIMITATION OF ABSTRACT	18. NUMBER OF PAGES	19a. NAME OF RESPONSIBLE PERSON
a. REPORT	b. ABSTRACT	c. THIS PAGE			Richard E. Huffman, Lt Col, USAF
U	U	U	UU	101	19b. TELEPHONE NUMBER *(Include area code)* (937) 255-6565, ext 7490 (richard.huffman@afit.edu)

Standard Form 298 (Rev. 8-98)
Prescribed by ANSI Std. Z39-18